Received: 25 February 2020 | Revised: 21 July 2020 | Accepted: 23 July 2020

DOI: 10.1111/mec.15588

ORIGINAL ARTICLE

MOLECULAR ECOLOGY WILEY

Pleistocene persistence and expansion in tarantulas on the Colorado Plateau and the effects of missing data on phylogeographical inferences from RADseq

Matthew R. Graham[1] | Carlos E. Santibáñez-López[1] | Shahan Derkarabetian[2] | Brent E. Hendrixson[3]

[1]Department of Biology, Eastern Connecticut State University, Willimantic, CT, USA

[2]Department of Organismic and Evolutionary Biology, Museum of Comparative Zoology, Harvard University, Cambridge, MA, USA

[3]Department of Biology, Millsaps College, Jackson, MS, USA

Correspondence
Matthew R. Graham, Department of Biology, Eastern Connecticut State University, Willimantic, CT 06226, USA.
Email: grahamm@easternct.edu

Funding information
National Science Foundation, Grant/Award Number: DEB-1754030

Abstract

Montane species endemic to the "sky islands" of the North American southwest were significantly impacted by changing climates during the Pleistocene. We combined mitochondrial and genomic data with species distribution modelling to determine whether *Aphonopelma marxi*, a large tarantula from the nearby Colorado Plateau, was similarly impacted by glacial climates. Genetic analyses revealed that the species comprises three main clades that diverged in the Pleistocene. A clade distributed along the Mogollon Rim appears to have persisted in place during glacial conditions, whereas the other two clades probably colonized central and northeastern portions of the species' range from refugia in canyons. Climate models support this hypothesis for the Mogollon Rim, but late glacial climate data appear too coarse to detect suitable areas in canyons. Locations of canyon refugia could not be inferred from genomic analyses due to missing data, encouraging us to explore the effect of missing loci in phylogeographical inferences using RADseq. Results from analyses with varying amounts of missing data suggest that samples with large amounts of missing data can still improve inferences, and the specific loci that are missing matters more than the number of missing loci. This study highlights the profound impact of Pleistocene climates on tarantulas endemic to the Colorado Plateau, as well as the mixed nature of the region's fauna. Some animals recently colonized from nearby deserts as glacial climates receded, whereas others, like tarantulas, appear to have persisted on the Mogollon Rim and in refugia associated with the region's famous river-cut canyons.

KEYWORDS

COI, ddRAD, MAXENT, Mygalomorphae, Southwest, spider

1 | INTRODUCTION

Pleistocene refuge theory has been central in the understanding of evolutionary diversification, current population genetic structure and the colonization of similar refugial habitats (Dynesius & Jansson, 2000; Graham et al., 1996). Some studies on arid-adapted vertebrates, plants and arthropods distributed in the Nearctic have shown a general pattern of divergence among populations facilitated by Pleistocene events, such as population fragmentation into separate climatic refugia (Angulo, Amarilla, Anton, & Sosa, 2017; Devitt, 2006; Douglas, Douglas, Schuett, & Porras, 2006; Licona-Vera, Ornelas, Wethington, & Bryan, 2018; Loera, Ickert-Bond, & Sosa, 2017). Locations of key Pleistocene refugia have been identified in North American warm deserts (Bell, Hafner, Leitner, & Matocq, 2010; Graham, Hendrixson, Hamilton, & Bond, 2015; Graham, Jaeger, Prendini, & Riddle, 2013a, 2013b; Graham, Wood,

Henault, Valois, & Cushing, 2017; Jezkova, Jaeger, Marshall, & Riddle, 2009; Myers et al., 2019), with less work carried out to identify persistent and stable habitats in adjacent cold-desert regions (but see Massatti & Knowles, 2014; Wilson & Pitts, 2012). Here, we set out to determine how Pleistocene climate fluctuations and potential refugia may have influenced arthropods endemic to the Colorado Plateau, a cold desert that adjoins several warm deserts (Chihuahuan, Mojave and Sonoran).

The Colorado Plateau is unique among the arid systems of western North America because it receives regular annual snow and subfreezing winter temperatures, similar to the cold Great Basin Desert to the west. The area also receives more rainfall than the North American deserts, averaging 136–668 mm of precipitation per year (Hereford, 2002), making it a semi-arid province (as defined by the aridity index of the World Atlas of Desertification). Roughly centred on the Four Corners region of the United States (Figure 1), the Colorado Plateau encompasses over 600,000 square kilometres of remarkably exposed and colourful plateaus and buttes, and famously deep river incisions like the Grand Canyon. Although generally thought to have occurred at sea level in the late Cretaceous, the modern surface of the plateau now averages about 2 km in elevation (McQuarrie & Chase, 2000; Pederson, Mackley, & Eddleman, 2002). As such, the region has experienced a rich geologic history since the Mesozoic.

Uplift of the Colorado Plateau is thought to have occurred in four pulses, beginning with the Laramide orogeny in the Late Cretaceous and ending with a Late Miocene–Holocene erosion event likely caused by contemporaneous surface uplift (reviewed in Cather, Chapin, & Kelley, 2012; Karlstrom et al., 2012). Data from thermochronology, river incisions and radiometric dating revealed rapid regional exhumation from 6 to 10 Ma, suggesting that much of the region's uplift (25%–50%) may have occurred during the last 10 Ma (Karlstrom et al., 2012). Climates fluctuated tremendously on the plateau during the Pleistocene, with increased precipitation and colder temperatures during glacial periods that favoured more mesic species assemblages. Xeric species are thought to have been restricted to lower elevations during glacial maxima, such as those of the Grand Canyon, and expanded up in elevation along canyon

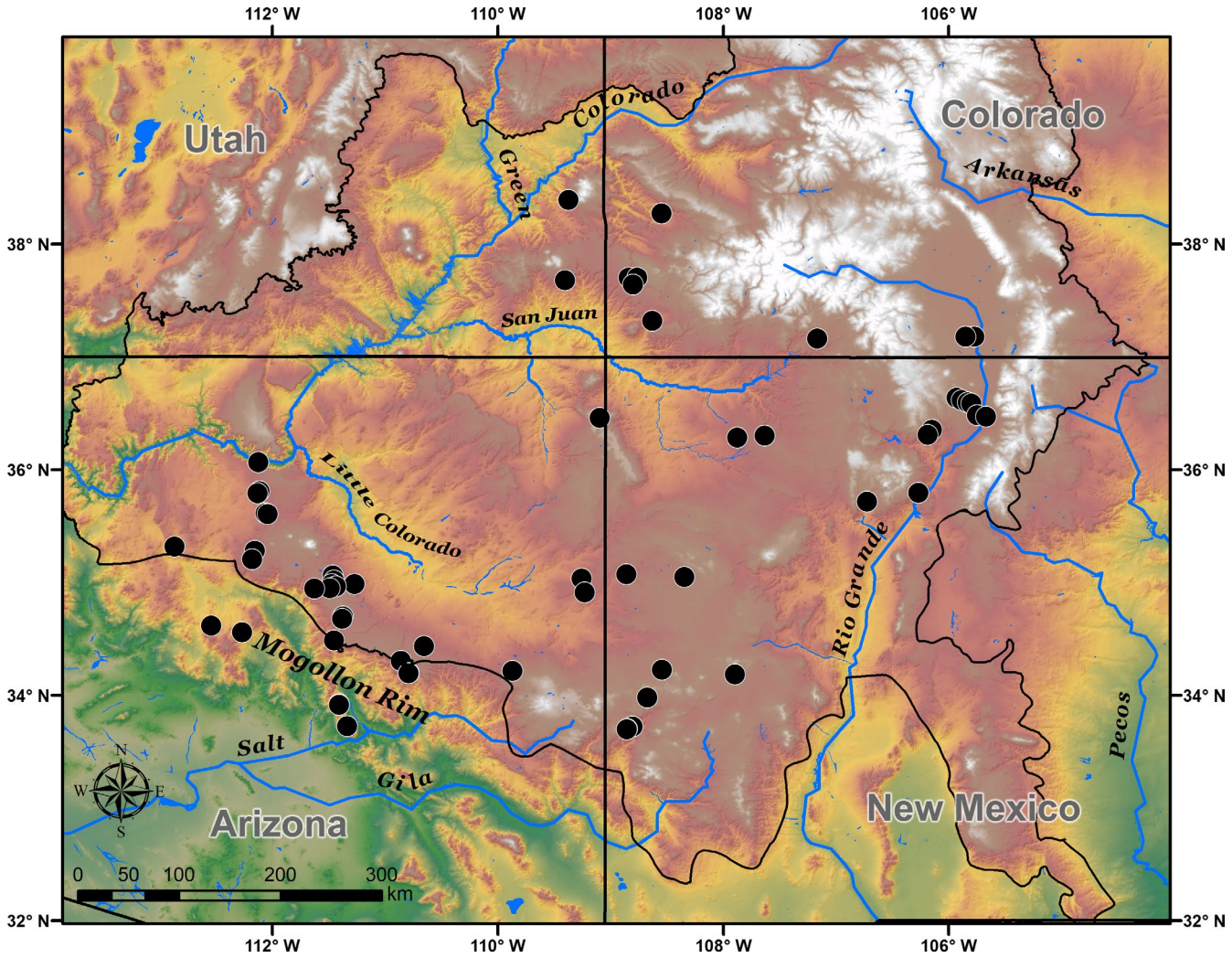

FIGURE 1 Map of the Colorado Plateau region (outlined in black) in the southwestern USA showing the distribution of *Aphonopelma marxi* samples used in this study (circles)

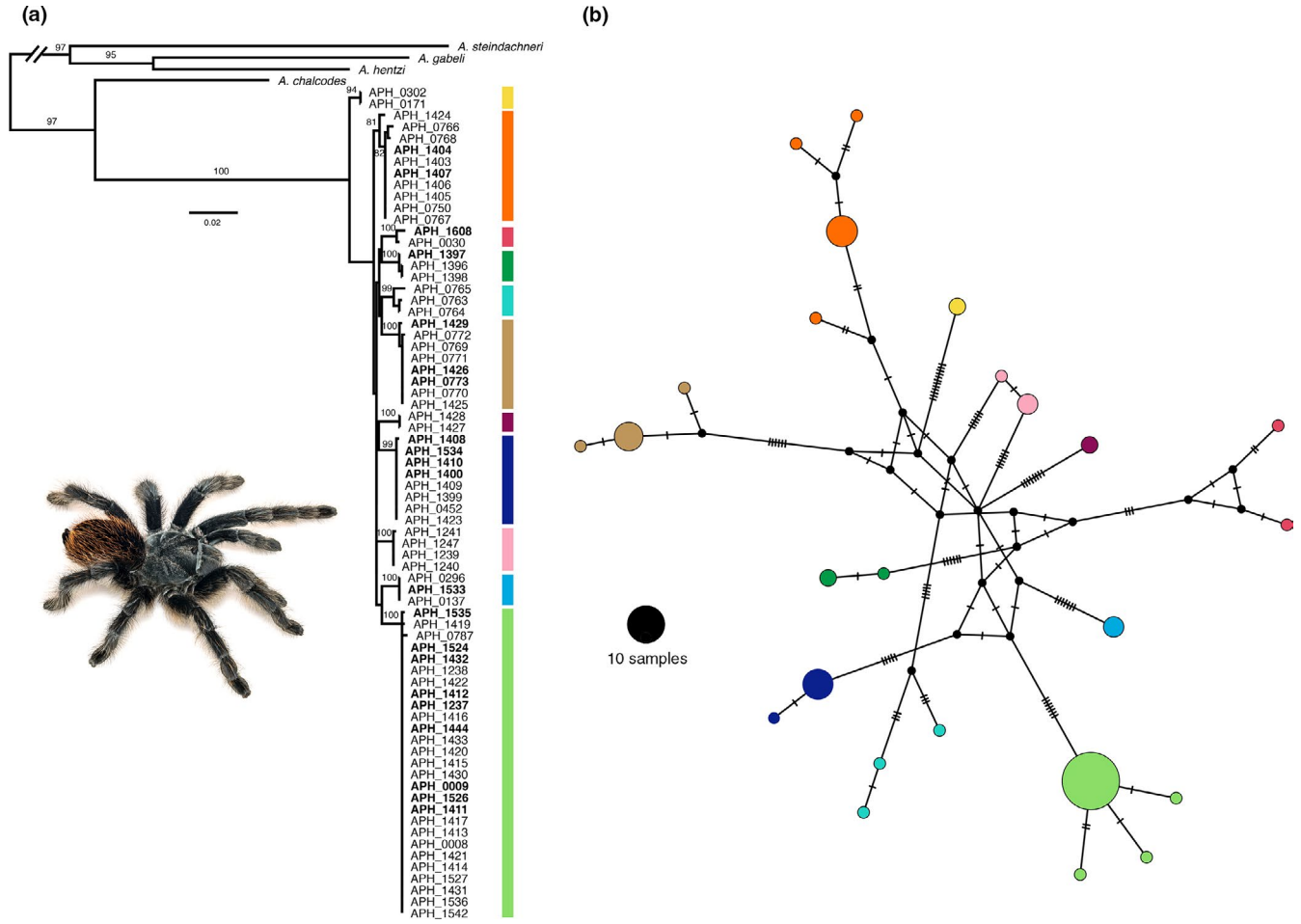

FIGURE 2 Phylogeographic patterns from mitochondrial samples (COI) from throughout the range of *Aphonopelma marxi*. (a) Maximum-likelihood (ML) phylogeny. Coloured bars indicate monophyletic clusters with bootstrap values above 80. Names of samples that were also used in RADseq analyses are in bold. (b) Median-joining network depicting relationships among haplotypes. Colours correspond to the ML phylogeny

corridors as climates warmed. Some species underwent large latitudinal shifts as well. These dramatic range changes are well illustrated by the distributions of plant macrofossils collected from packrat middens throughout the plateau (Betancourt, 1990; Coats, Cole, & Mead, 2008). For instance, during the most recent glacial episode (Wisconsinan), the Colorado pinyon pine (*Pinus edulis*) only grew along the southern portion of its current range, but quickly expanded northward over the Mogollon Rim of central Arizona and colonized most of the Colorado Plateau as climates warmed (Cole, Fisher, Ironside, Mead, & Koehler, 2013).

Genetic patterns from montane species throughout nearby "sky island" habitats suggest a strong influence of Pleistocene glacial cycles, with recent diversification events and range expansions for most species inhabiting the region (Knowles, 2000; Masta, 2000; Mitchell & Ober, 2013; Ober, Matthews, Ferrieri, & Kuhn, 2011; Smith & Farrell, 2005). Some montane arachnids, however, appear to have diversified prior to the Pleistocene (Bryson, Riddle, Graham, Smith, & Prendini, 2013; Derkarabetian, Burns, Starrett, & Hedin, 2016). While these studies do show interesting patterns, they are largely limited to taxa inhabiting higher elevations on sky islands that show relatively greater levels of isolation between genetic lineages. The effect of glacial cycles on taxa inhabiting the less isolated habitats at lower elevations, such as those found across the Colorado Plateau, is less understood. We suspect that species at lower elevations with limited dispersal capabilities, for instance, may have also been significantly influenced by Pleistocene climates despite increased connectedness among habitats.

We generated molecular data and climate-based distribution models for a tarantula endemic to the Colorado Plateau to determine whether Pleistocene climate fluctuations structured genetic diversity in arthropods found at lowerelevations. Also known as the "Grand Canyon black tarantula," *Aphonopelma marxi* is one of most striking invertebrates in the North American Southwest. This species is large, hirsute, and has a black to faded black body with numerous long orange to red setae on its abdomen (Figure 2). The species ranges throughout most of the mid to high elevations of the Colorado Plateau, including portions of Arizona, Colorado, New Mexico and Utah, as well as some isolated mountain ranges along the Mogollon Rim. Like most terrestrial tarantulas, *A. marxi* probably

has limited dispersal abilities and wandering males are responsible for the majority of gene flow.

Arthropods found at lower, nonmontane elevations on the Colorado Plateau could have responded to fluctuating climates in two ways. They could have persisted in their current distributions and adapted to different climatic conditions, or their distributions could have changed to track suitable climates. We refer to these as the "persistence" and "niche tracking" hypotheses, as described in a similar study on kangaroo rats in the nearby Great Basin Desert (Jezkova, Olah-Hemmings, & Riddle, 2011). Under the persistence scenario, we would expect *A. marxi* to exhibit limited population structure and genetic diversity attributable to isolation by distance, but with SDMs indicating a significant shift in the distribution of suitable habitat. Alternatively, the niche tracking hypothesis predicts that population structure will be associated with Pleistocene refugia, perhaps associated with river drainages that carved the region's major canyon systems (Figure 1). Demographic analyses should indicate that *A. marxi* populations have undergone recent expansions, and genetic diversity should be higher in areas that acted as refugia. In addition, higher genetic diversity should be found in areas identified as late glacial refugia by SDMs. Here, we set out to test these hypotheses using mitochondrial DNA, genomewide SNP data from restriction site-associated DNA sequencing (RADseq) and species distribution models (SDMs).

2 | MATERIALS AND METHODS

2.1 | Taxon sampling

We collected 72 individuals of *A. marxi* from throughout the species' range. Adult females and immature individuals were found by actively flipping rocks and searching for burrows which were excavated by hand. We collected males on roads and trails during their breeding season (late September through early November) when they wander in search of females. Two to four legs were removed from the right side of each specimen and stored in RNA*later* RNA Stabilization Reagent (Qiagen) at −80°C as a source of muscle tissue for DNA analyses. The remainder of each specimen was preserved as a voucher in 80% EtOH and deposited in the William F. Barr Entomological Museum in the Department of Entomology, Plant Pathology and Nematology at the University of Idaho in Moscow, Idaho. Genomic DNA was isolated from leg tissues using the DNeasy Tissue Kit (Qiagen) and stored at −20°C prior to PCR and sequencing. Locality data and personal identifiers for each specimen are provided in Table S1.

2.2 | Mitochondrial DNA sequencing

Using previous protocols (Hendrixson, 2019; Hendrixson, DeRussy, Hamilton, & Bond, 2013; Hendrixson, Guice, & Bond, 2015), we amplified a section of the mitochondrial genome coding for the cytochrome c oxidase subunit I (*COI*) gene using the C1-J-1715 "SPID" forward primer (5′-GAG CTC CTG ATA TAG CTT TTC C-3′) and C1-N-2776 reverse primer (5′-GGA TAA TCA GAA TAT CGT CGA GG-3′; Hedin & Maddison, 2001). We used 50 μl PCR cocktails containing the following: 27.25 μl ultra-pure water, 5 μl of each primer (2.5 pmol/μl; 250 nM final concentration), 0.25 μl (1.25 U) Takara ExTaq DNA polymerase, 5 μl ExTaq Buffer, 4 μl dNTPs; 2.5 μl bovine serum albumin (New England Bio Labs) and 1 μl genomic DNA. Thermal cycler conditions were as follows: 95°C for 2 min; 30 cycles at 96°C for 30 s, 48°C for 30 s and 72°C for 1 min; and a final extension at 72°C for 2 min. PCR products were cleaned of impurities using a 6:1 ratio of PCR product to ExoSAP-IT (GE Healthcare). Bidirectional sequencing was conducted with the cleaned amplicons on an ABI 3130 Genetic Analyzer with the ABI Big Dye Terminator ver. 3.1 Cycle Sequencing Ready Reaction Kit. We edited double-stranded DNA fragments manually in Geneious Pro ver. 4.8.5. The resulting *COI* alignment is hereafter referred to as "m1." Sequences were deposited in GenBank with Accession nos listed in Table S1.

2.3 | RAD sequencing and assembly

We selected 24 samples representing each of the 11 clades identified in the mitochondrial analyses (see Section 3) for additional analysis using RADseq. We prepared RAD libraries for dual-indexed sequencing using the 3RAD protocol (Glenn et al., 2017; Hoffberg et al., 2016). The method uses two restriction enzymes to cut DNA for adapter ligation but differs from traditional ddRADseq protocols by using a third restriction enzyme to cleave adapter dimers. In our protocol, we used EcoRI-HF and ClaI to make cuts for adapter ligations and MspI for dimer cleaving (all enzymes from New England Biolabs).

We simultaneously cleaved genomic DNA and ligated unique pairs of adapters (purchased from BadDNA, University of Georgia, Athens, GA) in 24 μl reactions containing 90 ng DNA, 3.3 μl master mix and 1 μl of each 5 μM adapter. We prepared the master mix so that each 24 μl reaction contained 30 units MspI, 30 units EcoRI-HF, 10 units ClaI and 1.7 μl 10x Cutsmart Buffer. The samples were incubated in a thermal cycler for 1 hr at 37°C. We prepared a ligase mixture containing the following for each reaction: 0.5 μl 10x Ligase Buffer, 146 units T4 DNA ligase, 1.5 μl 10 mM rATP and 2.95 μl ultra-pure water. 54 μl of the ligase mixture was immediately added to each sample while on the thermal cycler and subsequently incubated for at 22°C for 20 min and 37°C for two cycles and then at 80°C for an additional 20 min. Samples were then purified using a 1:1 mixture of AmPure XP magnetic beads (Beckman Coulter) and a 96-well ring magnet. We washed the samples using fresh 80% EtOH, let them air dry and resuspended in 25 μl TLE buffer.

Full-length 3RAD libraries were made using 3 μl of each sample to a pool. A 25 μl reaction was then made containing 5 μl of pooled DNA, 2.5 μl iTru5 primer, 2.5 iTru7 primer, 1x KAPA HiFi Fidelity Buffer, 0.3 mM of each dNTP and 0.5 units of KAPA HiFi Hotstart DNA polymerase. Samples were amplified using the following

thermal cycler profile: 95°C for 2 min; 17 cycles of 98°C for 20 s, 61°C for 15 s, 72°C for 30 s; and 72°C for 5 min. We cleaned the samples again by using a 2/3 ratio of template to AmPure beads, washed them twice with 80% EtOH and resuspended in 20 μl TLE. The samples were electrophoresed with a PippinHT (Sage Science) on a 1.5% agarose gel to size-select for 500-bp fragments (+/− 10%).

Library concentration was increased using 50 μl PCRs containing 20 μl of size-selected DNA, 5 μl of 5 μM P5 primer, 5 μl of 5 μM P7 primer, 0.3 mM of each dNTP, 10 μl 1x KAPA HiFi Fidelity Buffer and 1 unit of KAPA HiFi Hotstart DNA Polymerase. The DNA was amplified using the following thermal cycler profile: 98°C for 45 s, 98°C for 15 s, 60°C for 30 s, and 72°C for 60 s for 10 cycles; and 72°C for 5 min. Amplicons were cleaned with a 2/3 DNA to AmPure beads ratio, washed twice with 80% EtOH and resuspended in 32 μl ultra-pure water.

The PCR product was checked for quality using Bioanalyzer and then sequenced using 2 × 150 paired-end sequencing on a full lane of an Illumina HiSeq X at Admera Health. We checked the DNA concentrations of samples throughout the library preparation protocol using a Qubit 4 Fluorometer (Invitrogen).

Raw reads were assembled using the IPYRAD (Eaton, 2014) with the default parameters (cluster threshold = 0.95). We hereafter refer to this complete matrix as "m2" (including all constants and SNP sites), which we used to generate two smaller matrices, one which only included SNPs (hereafter "m3") and another that only include unlinked SNPs (hereafter "m4"). Three samples possessed mostly ambiguous or missing data and were eliminated from our analyses.

2.4 | Phylogenetic inference and divergence dating

Maximum-likelihood phylogenetic reconstruction on the four matrices (m1–m4) was conducted using IQTREE version 1.6.6 (Nguyen, Schmidt, von Haeseler, & Minh, 2014), implementing MODELFINDER (Kalyaanamoorthy, Minh, Wong, von Haeseler, & Jermiin, 2017) and ultrafast bootstrap resampling to gauge nodal support (Hoang, Chernomor, von Haeseler, Minh, & Vinh, 2018; Minh, Nguyen, & Haeseler, von, A., 2013). Bayesian inference analyses were also conducted on all matrices with MRBAYES version 3.2.7 (Huelsenbeck & Ronquist, 2001; Ronquist & Huelsenbeck, 2003; Ronquist et al., 2012) with 10 million generations sampling every 1,000 generation and a burn-in of 25%. Stationarity and ESS values were checked using TRACER version 1.7 (Rambaut, Drummond, Xie, Baele, & Suchard, 2018). TREEANOTATOR version 2 from the BEAST2 package (Bouckaert et al., 2014) was used to produce maximum clade credibility trees. Trees were visualized and exported in FigTree version 1.3.1 (Rambaut, 2008).

Divergence dates were estimated by analysing the *COI* and linked SNP data (m3) as separate partitions in a concatenated analysis with BEAST 1.8.0 (Drummond, Suchard, Xie, & Rambaut, 2012). We ran the analysis using best-fit substitution models for each partition (GTR for COI and HKY for RAD SNP determined as above), uncorrelated lognormal clock models for each gene and the coalescent constant size tree prior. We calibrated the molecular dating estimates by using a rate calibration for the COI partition that is commonly used in arthropods, including tarantulas (Graham et al., 2015; Papadopoulou, Anastasiou, & Vogler, 2010). We used a normal clock rate prior with mean rate (ucld.mean for COI) of 0.0169 substitutions per site per million years. We ran the software using four independent chains, each for 100 million generations and sampled every 10,000 steps. All operators were optimized automatically, and we confirmed effective sample size values were adequate (all >300) using TRACER 1.7. Note that although this rate has been broadly applied to arthropods, the actual rate for tarantulas could substantially differ, so divergence date estimates using our approach should be considered with caution.

2.5 | Demographic history

We calculated molecular diversity statistics, such as nucleotide diversity, and tested for evidence of recent demographic changes using Tajima's *D* (Tajima, 1989) and Fu's FX (Fu, 1997) with the COI data in Arlequin 3.5 (Excoffier, Laval, & Schneider, 2005). We visually explored the relatedness of COI haplotypes by creating a median-joining network in POPART (Population Analysis with Reticulate Trees) version 1.7.2 (Leigh & Bryant, 2015) using an ε value of 0. Changes in effective population size over time were assessed with Bayesian skyline plots and Bayesian skyride plots (Minin, Bloomquist, & Suchard, 2008) using the mtDNA data, implemented in BEAST for 100 million generations. We set the number of population size changes to 10 (the default) for the Bayesian skyline plots. Bayesian skyride plots do not require a priori estimates of the number of population size estimates. We ran the analyses using the previously determined substitution models, molecular clock calibrations and priors, each for 100 million generations. We also assessed the correlation between pairwise COI genetic distances and geographic distances in *A. marxi* using a Mantel test (10,000 permutations) implemented in XLSTAT version 2019.3.2 (Addinsoft). Pairwise genetic distances (uncorrected *p*) were calculated in MEGA version X (Kumar, Stecher, Li, Knyaz, & Tamura, 2018) and geographic distances with the Geographic Distance Matrix Generator version 1.2.3 (http://biodiversityinformatics.amnh.org/open_source/gdmg). A significant correlation between genetic and geographic distances implies a pattern of gene flow indicative of isolation by distance (IBD). Four separate IBD analyses were performed on the COI data set: one for every sample and one for each of the three main clades recovered in the RADseq phylogenetic analyses (see Section 3). Demographic analyses were not conducted with the RAD SNPs due to missing data.

2.6 | Population structure

Genetic population structure and admixture were analysed using the Bayesian Markov chain Monte Carlo (MCMC) clustering method as implemented in STRUCTURE version 2.3.3 (Pritchard,

Stephens, & Donnelly, 2000). These analyses were conducted using the matrices m3 (836 SNPs) and m4 (137 uSNPs), assuming correlated allele frequencies, without using prior population information and with the admixture and no-admixture models. We conducted 10 independent runs for each value of K (from 1 to 6) with 100,000 mcmc cycles and a burn-in of 10,000 iterations. The number of populations (*K*) best fitting the data set was defined using the log probabilities of *X*|*K* (Pritchard et al., 2000) and the DeltaK method (Evanno, Regnaut, & Goudet, 2005) implemented online in STRUCTURE HARVERSTER version 0.6.94 (Earl & vonHoldt, 2012). Subsequently, CLUMPP version 1.1.2 (Jackobsson & Rosenberg, 2007) with the greedy algorithm was used to align multiple runs of the selected *K* values from the previous step. Structure plots (Ramasamy, Ramasamy, Bindroo, & Naik, 2014) were used to visualize the population membership of the individual samples as bar plots.

Complementary to Bayesian clustering analyses, a discriminant analysis principal components (DAPC) was performed using the COI (m1) and the SNPs (m3) data sets. We constrained the values of clusters (k) to 3 (m3) and 8 (m1; as suggested by BIC values) using the first 7 (m1) or 10 (m3) PCs, with the package ADEGENET (Jombart, Devillard, & Balloux, 2010) in R 3.5.2 (R Core Team, 2018). All figures were edited in Adobe Illustrator. Using the SNPs, we studied population structure using a principal component analysis (PCA) with dudi.pca in the R package ADEGENT.

2.7 | Species distribution modelling

We developed species distribution models (SDMs) for *A. marxi* using GPS coordinates for the 72 samples, as well as 6 additional sites where we have collected the species. Location data associated with museum samples and literature records can be vague, and georeferencing is prone to errors, so we chose to conduct analyses using only our own coordinates. Using these data, we generated SDMs for *A. marxi* under current (1,950–2,000) and LGM (ca. 21 Ka) climatic conditions (CCSM4 simulations) using bioclimatic interpolations downloaded from the WorldClim database (Hijmans, Cameron, Parra, Jones, & Jarvis, 2005). The interpolation layers were available at 30′ (ca 1 × 1 km) resolution for current climates and 2.5′ (4 × 4 km) resolution for the LGM climates. All layers were clipped to an extent encompassing the known range of *A. marxi*, as well as adjacent, potentially accessible habitats (30–40° N and 102–116° W). To avoid overfitting, we screened all 19 bioclimatic layers in each data set for multicollinearity using ENMTOOLS 1.3 (Warren, Glor, & Turelli, 2010) and removed four variables (Bio1, Bio5, Bio10 and Bio13) that were highly correlated (Pearson's $r^2 > .8$) with two or more other variables. Five additional pairs of variables were still highly correlated, so we ran MAXENT 3.3.3k (Phillips, Anderson, & Schapire, 2006) using default settings, and removed one variable from each highly correlated pair (Bio3, Bio4, Bio6, Bio14 and Bio18) based on their relative contributions to the Maxent model. The following ten predictor variables were retained: Bioclim 2, 7, 8, 9, 11, 12, 15, 16, 17 and 19. We used ENMTOOLS to trim the occurrence data so that only one point was retained per 30' grid cell to reduce sampling bias.

Using the 10 Bioclim layers and spatially filtered occurrence data, we ran MAXENT again to construct a present-day SDM and then projected it to the LGM climatic conditions. We ran the analysis using five replicates for cross-validation (equivalent to 20% testing), logistic output, the maximum number of iterations set to 10,000 and a random seed. The default regularization parameter can negatively influence models (Elith et al., 2011; Merow, Smith, & Silander, 2013). Therefore, we optimized the regularization multiplier by generating models with values from 1 to 10 and chose the value with the best Akaike information criterion (AIC_c) score (a multiplier of 3). All other parameters were set to default.

The logistic output, which is a continuous probability of presence ranging from 0 to 1, was displayed in ARCGIS 10.1 (ESRI). We omitted areas where climates were unsuitable by using the "minimum training presence" threshold, an option that sets the omission rate to zero. This threshold is appropriate because we only used coordinate data from occurrence records that we collected ourselves, rather than estimated (georeferenced) records.

2.8 | Analyses of missing data

The effect of missing data has been observed in phylogenetic reconstruction and population genomics in several studies suggesting different impacts (Huang & Knowles, 2016; Lal, Southgate, Jerry, & Zenger, 2016; Leaché, Banbury, Felsenstein, De Oca, & Stamatakis, 2015; O'Connell & Smith, 2018; Shafer et al., 2017), such as the construction of populated genetic maps (Konar et al., 2017). Here, our results showed contrasting phylogenetic relationships with population membership of some samples, especially those with more missing data. To address this issue, we calculated the amount of missing data of each matrix using the MatrixCondenser algorithm (de Medeiros & Farrell, 2018) and eliminated all samples with more than 65% missing data (m6–8), and with more than 30% missing data (m9–11). New phylogenetic, structure and DAPC analyses were conducted for these new matrices using the same procedures described above.

3 | RESULTS

3.1 | DNA sequence data

Mitochondrial COI sequences resulted in a matrix consisting of 72 individuals, plus 4 outgroups and 894 nucleotide sites (m1). High-throughput sequencing of RAD amplicons generated a total of 50,425,176 reads obtained from 24 individuals of *A. marxi* (mean = 2,101,049, *SD*+- = 2,750,945). After data processing, less than 4% of the consensus reads were kept with an average of 92 loci assembled for each individual. Reads from three individuals

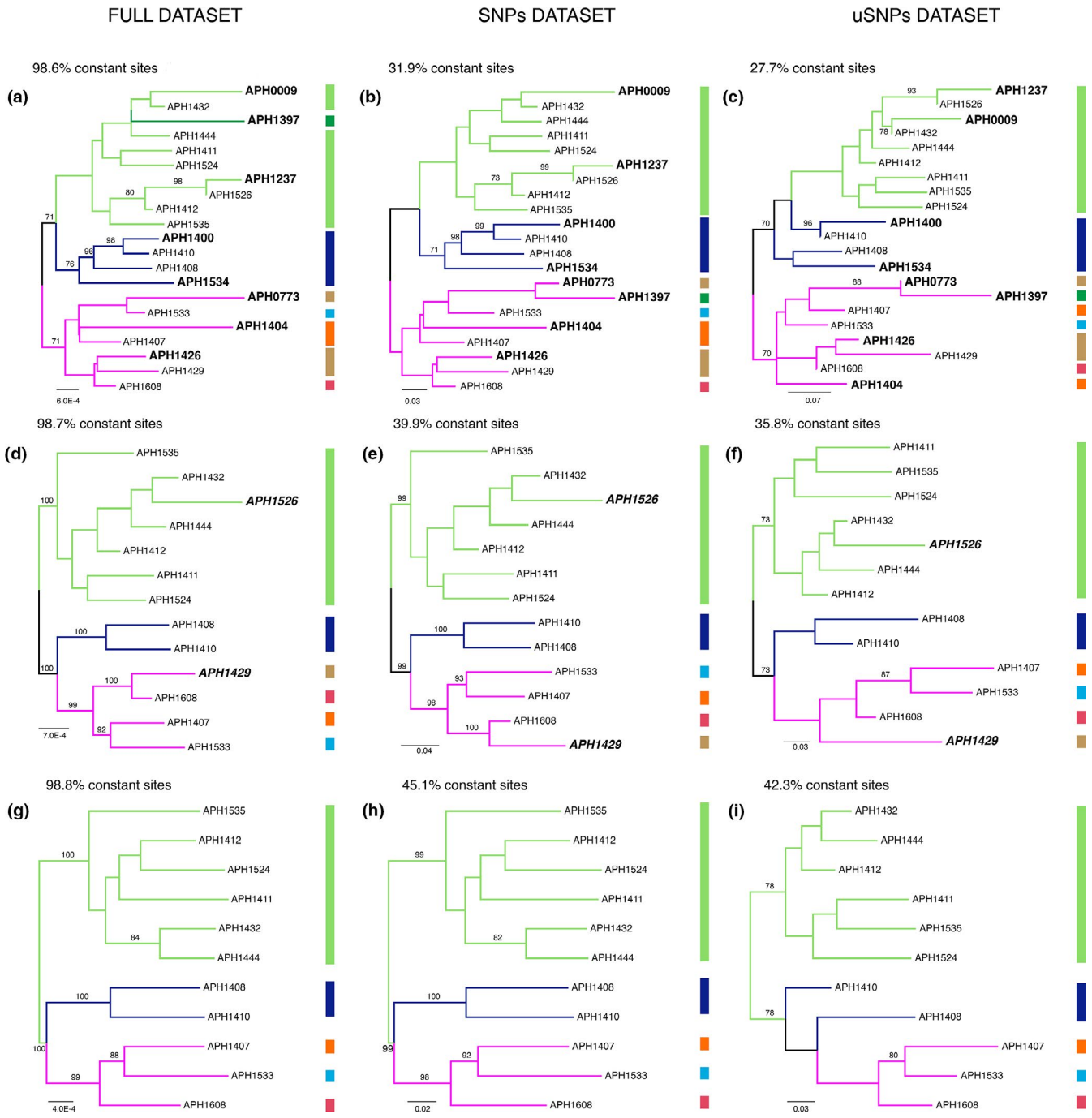

FIGURE 3 Alternative maximum-likelihood phylogenies generated using RADseq data sets with different amounts of missing data. The top row (a–c) shows phylogenies produced using all 21 individuals, the middle row (d–f) shows those for 13 samples with the least missing data, and the bottom row (g–i) shows phylogenies for 11 samples with the least missing data. Phylogenies in the left column (a, d, g) were generated using the full data set, the middle (b, e, h) with the full SNP data set and the right column (c, f, i) with the unlinked SNP data set. Accordingly, the phylogeny on the top left represents the most missing data and the one on the bottom right the least. Branch colours indicate membership assignments from structure analysis as presented in Figure 4. Matrix metrics are provided in Table S2.

(APH0452, APH1405 and APH1417) did not yield any loci and were eliminated from downstream analyses. The data sets obtained from ipyrad with at least 12 individuals per locus contained 836 and 137 SNPs and uSNPs, respectively. Concatenated matrices consisted of 21 individuals and 39,921 (m2), 836 (m3) and 137 (m4) nucleotides.

3.2 | Phylogenetic inference and divergence dating

Maximum-likelihood analysis of mtDNA (m1, Table S2) supported the monophyly of the 72 samples of *A. marxi* (Figure 2a). Two clades were recovered within the phylogeny, one (supported by high nodal values) grouping two individuals (APH0302, APH0171) and one

including 70 samples (not strongly supported). This second clade was further subdivided into 10 highly supported clades; however, relationships between these clades were not strongly supported (Figure 2a). Bayesian inference recovered a similar topology with strong support for the two main clades and 10 additional clades. Relationships among the 10 additional clades were again unresolved.

Maximum-likelihood analysis of RADseq (m2, Table S2) recovered the presence of three clades with ultrabootstrap support values slightly above 70% (Figure 3). These three clades consisted of individuals recovered in eight clades in the mitochondrial phylogeny (Figures 2a and 3a). A clade containing samples from the centre of the species' range (hereafter known as Central clade) was recovered with 76% bootstrap support and was sister to a clade containing samples from the northeastern part of the range (hereafter the Northeast clade). The Northeast clade was not recovered as monophyletic as in the COI phylogeny due to the inclusion of one sample (APH1397). Samples from the Mogollon Rim region in the southwestern portion of the species' range (hereafter the Southwest clade) formed a clade with 71% bootstrap support. The clade was recovered as the sister group to the other two clades and consisted of seven individuals, members of five different mitochondrial clades (Figure 3a). In contrast, ML analysis of m3 (Table S2) recovered the same topology, but only the Central clade had low branch support (71%; Figure 3b), and APH1397 was recovered as part of the Southwest clade (albeit with poor support). Lastly, ML analysis of m4 (Table S2) recovered two clades with low node support: one consisting of members of the Central (paraphyletic) and Northeast (monophyletic) clades, with the last one grouping members of the Southwest clade (Figure 3c).

Bayesian inference (BI) of m2–4 recovered highly similar topologies. BI of m2 recovered the three clades as monophyletic with strong support only for the Central clade. In contrast, BI of m3 recovered APH1397 as a member of the Northeast clade (contrary to previous analyses), although node support was low. Lastly, BI of m4 recovered the Central clade paraphyletic due to the exclusion of APH1534, with poor support for the monophyly of the other two clades.

The topology resulting from the BEAST analysis (Figure S2) was mostly identical to the topologies from ML and BI. Mean estimates indicate that *A. marxi* shared a common ancestor with *Aphonopelma chalcodes* in the late Pliocene (ca. 2.9 Ma). The time to the most recent common ancestor (TMRCA) for all of the *A. marxi* samples in this study were estimated to be in the mid-Pleistocene (ca. 1 Ma).

3.3 | Demographic history

Haplotype and haplotype diversity were much higher for the Southwest clade than the Central and Northeast clades (Table 1). Tajima's *D* and Fu's F_S were significantly negative for the Northeast clade, in accordance with a model of population expansion. Tajima's *D* was negative, but not significantly negative, for the Southwest clade. Fu's F_S was positive for the Southwest clade (Table 1). The Central clade possessed only two haplotypes and one polymorphic site, which the Bayesian skyline and Bayesian skyride plots both showed a general decrease in effective population size in the late Pleistocene, followed by a recent increase (Figure S3). These changes in effective population size are similar to fluctuations in global temperatures, as estimated for ocean surface temperatures (Hansen, Sato, Russell, & Kharecha, 2013). The Bayesian skyride plot predicted an additional brief increase in effective population size beginning approximately 125 Ka, followed by a decrease. This trend roughly matches the change in global temperatures following the Illinoian glacial episode, which ended 130 Ka. The correlation between pairwise COI genetic and geographic distances for the entire data set was significant ($r = .471$, $p < .0001$), in accordance with a pattern of gene flow due to isolation by distance. However, when analysed separately, only the Southwest clade showed a significant correlation between genetic and geographic distances (Table 1); the insignificant correlation between genetic and geographic distances for the Central and Northeast clades is more consistent with a pattern of recent population expansion.

3.4 | Population structure

Structure analyses of the SNPs (m3) with admixture and no-admixture models found a that $K = 3$ was optimal, splitting *A. marxi* into three distinct genetic clusters. This is in partial agreement with the clades

TABLE 1 Summary statistics for COI data for three main clades of *Aphonopelma marxi* defined by RADseq analyses. Individuals from clades that were not represented in the RADseq data set were excluded. The Central clade was excluded from demographic analyses due to its small sample size

Clade	*n*	*H*	*h*	π	*s*	*D*	*F*	*r*
Northeast	27	4	0.214 (±0.103)	<0.001	4	−1.888*	−2.509**	.002
Central	8	2	<0.001	<0.001	1	–	–	−.213
Southwest	26	12	0.877 (±0.043)	0.012 (±0.006)	43	−0.098	1.552	.663***

Standard deviations are in parentheses.

Abbreviations: *D*, Tajima's D; *F*, Fu's F_S; *h*, haplotype diversity; *H*, number of different haplotypes; *n*, number of individuals; *r*, Pearson's correlation coefficient for tests of IBD; *s*, number of polymorphic sites; π, nucleotide diversity.

*$p < .05$;

**$p < .001$;

***$p < .0001$.

recovered in phylogenetic analysis of the RADseq data (Figure 4). Two individuals (APH1404 and APH1397, both with >80% missing data) had different genetic membership to two different clusters depending on the model used (Figures 2a and 4a). In contrast, the structure analyses of the uSNPs (m4) with the no-admixture model found an optimal *K* value of 5, whereas the admixture model found a *K* value of 3 optimal (Figure 4a). There is no congruence between these two analyses with the previous results shown above. This discordance suggests that the grouping of individuals with high missing data values changes between different genetic clusters (see missing data section below).

Discriminant analysis of the principal components (DAPC) of the mitochondrial data favoured the presence of eight clusters (Figure S4). These clades partially agreed with those recovered in the mitochondrial topologies and their geographic distribution (Figure 5a–c). In addition, DAPC of the RADseq favoured three clusters (Figure S5) with some differences between the phylogenetic topologies and geographic distribution (Figure 5b,d). The Central clade in this analysis consisted of only two individuals (APH1140 and APH1408), whereas the Northeast clade included 12 individuals (three more than those recovered in other of our analyses; Figure 5b).

3.5 | Species distribution modelling

The average AUC score for the test data was 0.944 (*SD* = 0.022), showing that the SDM performed significantly better than random. The LGM model (Figure 6a) depicts a much-reduced distribution for *A. marxi* during the height of the Wisconsinan glaciation. Only the southwestern portion of the species' current range along the Mogollon Rim and some areas along the Arizona/Mexico border appear to have been suitable for these spiders during the LGM. Most of the species' present-day range appears to have been unsuitable during the LGM. Although the SDM shows a considerable reduction in range during the LGM, the majority of the highlighted habitat is depicted as highly suitable.

The SDM representing present-day climates (Figure 6b) shows suitable habitat across most of the mid to high elevations of the Colorado Plateau. Climatic suitability is highest in the southwest along the Mogollon Rim, along the Arizona/New Mexico border in the San Francisco, Zuni and Chuska mountain ranges and along the New Mexico/Colorado border in the San Juan Mountains. Additional suitable climates are located outside the known range of *A. marxi* west of the Rio Grande in the Sangre de Cristo Mountains of New Mexico and Colorado, as well as north of the Colorado River in the mountains of southwestern Utah. This pattern is similar to that of the harvestman *Sclerobunus robustus* (Derkarabetian et al., 2016). The lower elevation habitats around the Colorado, Little Colorado and San Juan rivers are depicted as unsuitable.

3.6 | Analyses of missing data

Ten of the 21 samples in our RADseq analyses had more than 35% missing data; four from the Northeast clade, four from the Southwest clade and two from the Central clade (Figure 7a). After removing these samples, ML analyses of m6, 7, 9 and 10 (Table S2) recovered the Northeast clade as monophyletic (with high support) and sister group to the Central and Southwest clades (also strongly supported; Figure 3d,e,g,h). ML of m8 recovered the same relationship of the three clades, but with poor support, the Central and Southwest clades were not supported by bootstrap values higher than 70%. Lastly, ML analysis of m11 did not recover the monophyly of the Central clade (Figure 3i). Incidentally, to test the effect of the presence/absence of these samples on nodal support for the three different clades, we removed one terminal at a time, to create eight additional matrices (m12–19, Table S2, Figure 7a). The densest matrix (m9 = 11 individuals) recovered the three clades (Northeast, Central and Southwest) as monophyletic with high branch support (Figure 7b). These branch support values decreased as missing data increased with the inclusion of one individual at a time (from 12 to 21 individuals; Figure 7b).

Similarly, the membership of two samples (APH1400 and APH1534) recovered by DAPC of the additional eight matrices was not concordant their phylogenetic position (Figure 7c). Lastly, our structure analyses of matrices m7, 8, 10 and 11 (Figure 4b,c) suggested the presence of three clusters (Northeast, Central and Southwest clades) or five when the unlinked SNPs (uSNPs) were analysed using the no-admixture model. The percentage of membership of five of the high missing data samples to each of these clades fluctuated accordingly to the model used (Figure 7d). Interestingly, missing data showed little effect on the groupings of three samples (Figure 7d).

4 | DISCUSSION

4.1 | The effect of missing RADseq data on phylogeographic inference

One shortcoming of the RADseq approach in phylogenetic reconstruction is the large amounts of missing data produced (Leaché & Oaks, 2017), which increases with the number of loci sampled (Wagner et al., 2013). Missing data in such analyses are thought to be the result of data collection methods (summarized in Leaché & Oaks, 2017), bioinformatic processing of data assembly (Chattopadhyay, Garg, & Ramakrishnan, 2014; Shafer et al., 2017) and the threshold selected by researchers (Huang & Knowles, 2016). The use of full RAD sequences (SNPs with invariant sites) is often favoured in phylogenetic analyses to increase branch length and topological accuracy (i.e. Leaché et al., 2015). With the exception of the phylogenetic position of one taxon (APH1397 with almost 84% of missing data), our results agreed with these previous studies. Surprisingly, one sample (APH1400) was only represented by 10 loci (93.5% missing data), but its phylogenetic position was stable throughout almost all analyses (Figures 3 and 6). In contrast, the phylogenetic position of a sample with 25 loci (APH1397) differed among analyses.

The effect of missing data on assessments of population structure was significant. Pritchard, Wen, and Falush (2010) recommend

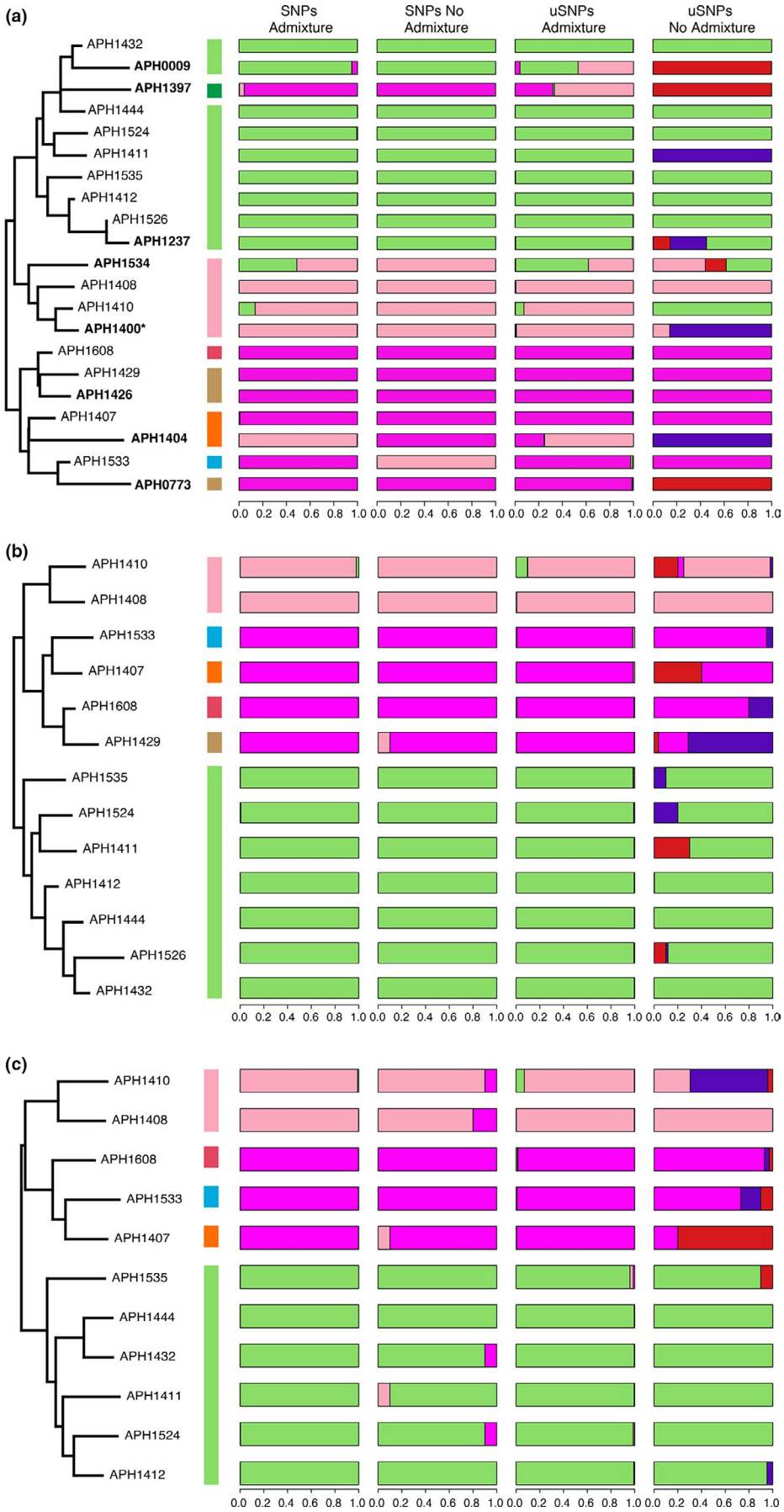
(a)
SNPs Admixture
SNPs No Admixture
uSNPs Admixture
uSNPs No Admixture
APH1432
APH0009
APH1397
APH1444
APH1524
APH1411
APH1535
APH1412
APH1526
APH1237
APH1534
APH1408
APH1410
APH1400*
APH1608
APH1429
APH1426
APH1407
APH1404
APH1533
APH0773
0.0 0.2 0.4 0.6 0.8 1.0
(b)
APH1410
APH1408
APH1533
APH1407
APH1608
APH1429
APH1535
APH1524
APH1411
APH1412
APH1444
APH1526
APH1432
(c)
APH1410
APH1408
APH1608
APH1533
APH1407
APH1535
APH1444
APH1432
APH1411
APH1524
APH1412

FIGURE 4 Maximum-likelihood phylogenies in relation to membership assignments based on structure analyses using alignments with different amounts of missing data using models with and without admixture: 21 sequences (a), 13 sequences (b) and (c) 11 sequences. Bars are coloured to correspond with clades recovered by the ML phylogenies (Figures 2 and 3)

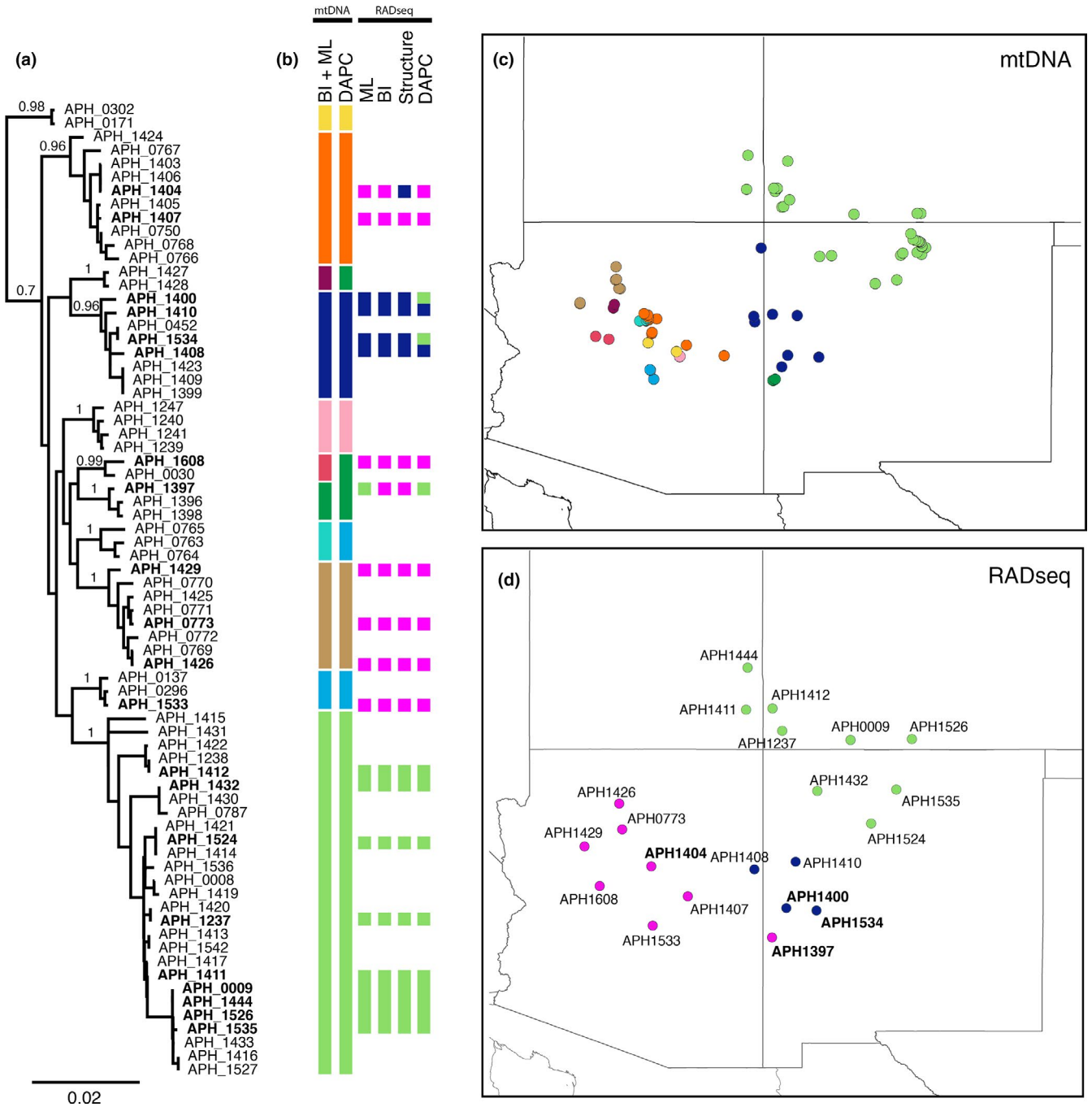

FIGURE 5 Phylogeographic patterns for *Aphonopelma marxi*. (a) Bayesian phylogeny generated using the mitochondrial data set. Samples in bold were used in RADseq analyses. (b) Group membership assignments based on different analyses of mitochondrial and RADseq data. (c) Distribution of mitochondrial samples coloured by phylogenetic clades based on ML (Figure 2) and Bayesian analyses. (d) Distribution of samples used in the RADseq analyses, coloured by ML clade based on the 9 phylogenies Figure 2

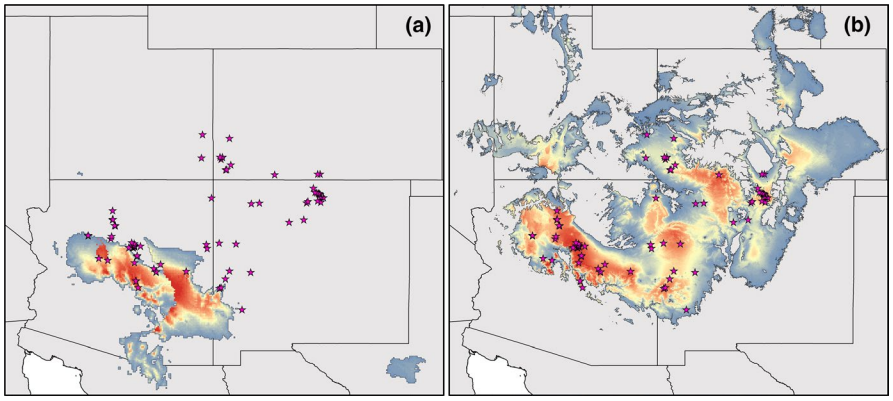

FIGURE 6 Species distribution models for *Aphonopelma marxi* projected onto late glacial (a) and current (b) climatic conditions. Stars represent localities used to generate the models. Areas with suitable climates are presented from low suitability (cool colours) to high suitability (warm colours)

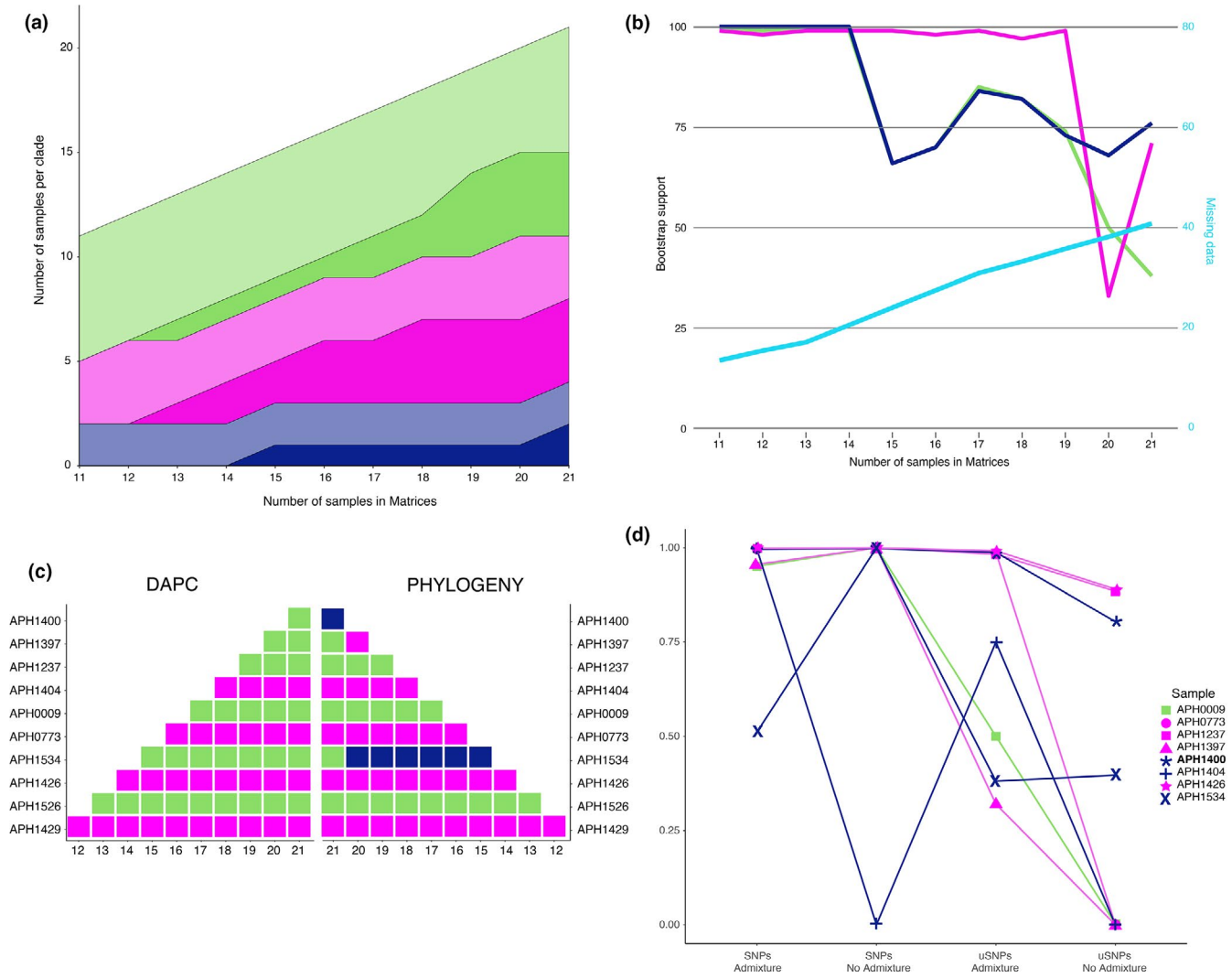

FIGURE 7 The effect of missing RADseq data on phylogenetic and population structure analyses. (a) Histogram showing the clade membership for samples based on 11 MI phylogenies generated using different alignments with different amounts of missing data. Clades are corresponding to those in Figure 3. Light colours represent samples with less than 40% missing data. (b) Bootstrap support values for the three main clades recovered in the 11 phylogenies generated with different amounts of missing data. The per cent missing is indicated in light blue. (c) Membership of the 10 taxa (with more than 40% of missing data) to the three main clades based on DAPC analysis of SNPs (left) and the phylogeny (right). (d) Membership percentages for 10 taxa with greater than 40% missing data as recovered by the structure analysis. Sample 1,400 with the highest amount of missing data is highlighted in bold

including samples with high amounts of missing data, even though estimates of ancestry from genetic clusters (Q) can be less accurate. In our analyses, the confidence in membership values varied considerably among five taxa with large amounts of missing data (Figure 7d). Our results showed that the variation in membership assignments could be attributed to ongoing or recent gene flow, but in our case, we find it more likely a product of missing data. Thus, we recommend that structure analyses using high amounts of missing SNP data should be interpreted cautiously.

Finally, the effect of missing data in DAPC was similar to its influence on phylogenetic analyses. In our DAPC analyses (Figure 7c), the results did not change when samples with missing data were consecutively added. Thus, our results again suggest that phylogeographic analyses with missing SNP data should be interpreted cautiously. Specifically, when data are missing in RADseq studies, it is important to explore them using a multipronged approach.

4.2 | RADseq data reveal population genetic structure in *A. marxi*

By combining phylogenetic, structure and DAPC analyses, we were able to determine which of the missing data samples still contained informative loci and SNPs, and were able to come to a consensus on our phylogeographical inferences. Importantly, without our RADseq samples, we would not have determined that *A. marxi* consists of three main genetic clades, as the analyses of the mtDNA suggest 11 different clades. This mito-nuclear discordance occurs among samples in the Southwestern clade along the Mogollon Rim, a topographically complex region severed by canyon systems and habitat differences (Figure 1). Various mechanisms have been proposed to explain mito-nuclear discordance in other animals (reviewed in Toews & Brelsford, 2012), but we hypothesize that topographic complexity could be acting as a filter, permitting nuclear gene flow by dispersing males, but inhibiting or reducing the flow of maternally inherited mtDNA in less vagile females. Although both sexes disperse, male tarantulas are well known for their dramatic fall "migrations" (Janowski-Bell & Horner, 1999; Stoltey & Shillington, 2009), which perhaps provide enough individuals travelling over large distances to occasionally or regularly overcome landscape barriers. Additional fine-scale sampling across the Mogollon Rim could test this hypothesis. Overall, the discordance among our data further emphasizes the importance of including RADseq samples when making phylogeographical inferences, even when they contain large amounts of missing data. Such results, however, should be interpreted cautiously.

4.3 | Tarantula response to changing Pleistocene climates

Analyses of mtDNA and genomic data revealed considerable phylogeographic structure that originated during the Pleistocene. Variation in the COI data suggests that *A. marxi* consists of 10–11 matrilineal clades, the majority of which are narrowly distributed along the Mogollon Rim (Figure 2). Two clades, however, inhabit the larger central and northeastern portions of the distribution, referred herein as the Central and Northeast clades, respectively. Our numerous phylogenetic and structure analyses of the RADseq data (see Missing Data section) collectively support a scenario of three main clades for *A. marxi*, the Northeast and Central clades as identified by the mtDNA, and the Southwest clade along the Mogollon Rim comprised of individuals that belong to the nine remaining mtDNA clades (Figures 2, 4 and 5).

This arrangement of genetic diversity is the antithesis to a more random distribution expected if Pleistocene climate fluctuations had little impact on the species. Specifically, haplotype diversity would have been spread more evenly across the plateau, with variation increasing with distance between samples (isolation by distance). Alternatively, the genetic diversity could be structured along barriers to gene flow, such as rivers. Interestingly, the range of *A. marxi* is largely circumscribed by rivers, so water barriers must impede the species from colonizing areas outside of its current distribution, such as the uninhabited expanses of suitable climate identified by our current SDM (Figure 6b). Within the species' range, however, evidence of gene flow restricted by rivers is not as clear.

In the Four Corners region, the Northeast and Central clades appear to be isolated from each other by potentially inhospitable habitat at lower elevations along the San Juan River. Further upriver to the east, however, identical Northeast clade haplotypes are found on both sides of the river. Similarly, low elevations surrounding the Little Colorado River seem to isolate Southwest clade populations from the Central clade. Tributaries of the Little Colorado River bisect populations within the Central clade, with identical haplotypes found on each side. Thus, rivers may indeed act as barriers to gene flow to tarantulas at lower elevations, supporting a "riverine barrier hypothesis" as proposed for studies on Opiliones (Hedin & McCormack, 2017; Thomas & Hedin, 2008). At higher elevations on the plateau, however, rivers do not significantly impede gene flow, like the "leaky" barrier scenario used to recently describe the nearby lower Colorado River (Dolby, Dorsey, & Graham, 2019).

Demographic analyses using the mtDNA data indicate that *A. marxi* underwent a recent population expansion (Figure S3). Additionally, the Northeast clade forms a star-shaped pattern in the haplotype network (Figure 2), which is often indicative of recent range expansion (Avise, 2000). Although the result may be hindered by a smaller sample size, the Central clade shows a similar pattern in the network. Summary statistics and demographic tests using the COI data show that the Central and Northeast clades possess low genetic diversity, a common outcome of Pleistocene refugia (Boyer, Markle, Baker, Luxbacher, & Kozak, 2016; Carnaval, Hickerson, Haddad, Rodrigues, & Moritz, 2009), and likely underwent recent spatial or demographic expansions (Table 1). Taken together, we suspect that the Northeast and Central clades are a result of a Pleistocene bottleneck followed by a recent range expansion. These results agree with predictions of our "niche tracking" hypothesis, which states that *A. marxi* colonized much of the Colorado Plateau

from glacial refugia. Specifically, we predicted that the distribution of the species followed shifting niche space from areas of suitable habitat along river-cut canyons where populations persisted during cooler and wetter glacial periods. Unfortunately, the Central clade only contains two mtDNA haplotypes and the Northeast only has four, so there is not enough variation to determine the direction in which each clade expanded their ranges. Furthermore, given considerable amounts of missing data in the RADseq alignments, we cannot effectively determine colonization routes by heterozygosity values either. Both clades, however, are located adjacent to major river systems where they could have existed during glacial maxima.

If the "niche tracking" hypothesis is plausible, then SDMs projected onto climatic simulations during the LGM should identify refugial areas of suitable habitats along the river valleys. Strikingly, our LGM SDM (Figure 6a) shows suitable habitat throughout most of the Mogollon Rim, essentially covering the range of the Southwest clade, but shows no suitable habitat throughout the rest of the species' range. This result is exactly what we would predict for the region inhabited by the Southwest clade. With nine mtDNA lineages originating in the mid-Pleistocene (Figure 2; Figure S1) and considerable phylogenetic structure in the RADseq data (Figure 3), we would expect that climates remained suitable throughout the Mogollon Rim region during the Pleistocene. On the contrary, the Central and Northeast clades show signatures of recent range expansion (Figure 2), and our demographic analyses indicate that these expansions probably occurred as climates warmed following the last glacial episode. If true, then we would expect the SDM to predict less suitable habitat in those areas during the LGM. The complete lack of suitable habitat in the LGM model, however, was unexpected (Figure 6a). The clades must have expanded from somewhere.

One could argue that perhaps the Central and Northeast clades recently colonized their respective areas from habitats predicted as suitable in the southwest. If true, we would expect to see low haplotype diversity in recently colonized areas, especially with increased distance from the source area in the southwest. Additionally, we would expect haplotypes to be identical or nearly similar to some of the haplotypes on the Mogollon Rim region because tarantulas disperse by walking (Reichling, 2000) rather than "ballooning" like some other mygalomorph taxa (see Coyle, 1983); therefore, these spiders should follow the gradual expansion and leading-edge models of colonization (reviewed in Koizumi, Usio, Kawai, Azuma, & Masuda, 2012; Jezkova et al., 2011). In other words, genetic diversity should be greater among older populations than among populations from regions that have been recently colonized.

We surmise that the SDMs are not wrong, but that the LGM climate layers are too course to recognize narrow areas of suitable climate along topographically complex regions. River-carved canyons such as the Grand Canyon, for instance, contain areas with dramatic changes in elevation, which influences climate. The LGM layers used in our analyses were at approximately 5-km^2 resolution. This means that climates were averaged across the landscape in 5-km^2 patches. Climates in canyons, however, can differ significantly in such a space. We suspect that the Central and Northeast clades expanded out of small areas of suitable habitats associated with river-carved canyons, which were not detectable by our LGM model. Contraction into small areas of suitable habitat along canyons would cause genetic bottlenecking and would explain why both clades contain such little genetic diversity. In hindsight, the complete lack of suitable habitat during the LGM might be what we should have predicted given the resolution of the climatic layers.

Despite large amounts of missing data, the genomic analyses allowed us to establish that *A. marxi* contains three major clades. Using the mtDNA from the individuals of these three clades, we showed that one had high levels of genetic diversity (where the species persisted during glacial periods), and two had extremely low diversity probably due to climate-driven bottlenecking (Table 1). The genomic data were not able to determine the relationships among the three clades, which changed depending on the data matrix or amount of missing data used. However, poor resolution among the major clades could mean that they diverged at about the same time, which from our analyses must have occurred sometime in the mid-Pleistocene. Interestingly, our mtDNA data set allows us to conclude that *A. marxi* fits the "niche tracking" hypothesis, as it appears to have tracked its niche during the Pleistocene, causing the species to diverge into three clades, two of which bottlenecked during the LGM and expanded back out onto the Colorado Plateau as climates warmed. Interestingly, this scenario is similar to that found for related *Aphonopelma* species from western North America which also appear to have fragmented during Pleistocene glacial conditions with subsequent range expansions (i.e. Hamilton, Formanowicz, & Bond, 2011).

Few other phylogeographic studies have centred on taxa endemic to the Colorado Plateau or addressed questions about the influence of Pleistocene climates in the region. However, an early study (Lamb, Jones, & Wettstein, 1997) determined that Pleistocene climate fluctuations "profoundly and repeatedly" influenced genetic patterns among populations of tassel-eared squirrels (*Scirurus aberti*) endemic to montane forests on the plateau. A more recent study, also using RADseq and SDMs, found that montane harvestman (*Sclerobunus robustus*) was likely restricted to two refugia (Derkarabetian et al., 2016). Interestingly, one refugium occurs in the San Juan Mountains and another along the Mogollon Rim, similar to the locations of the Southwest and Northeast clades we recovered in *A. marxi*. Although mean date estimates place the harvestman refugia in the Pliocene, uncertainty around the estimates extends into the Pleistocene. Thus, high-elevation species (*S. aberti* and *S. robustus*) and mid-elevation species (*A. marxi*) may have responded similarly to unstable climates throughout the Colorado Plateau.

Unlike *A. marxi*, which represents a unique endemic lineage of tarantulas (Hamilton, Hendrixson, & Bond, 2016), most other phylogeographical studies on Colorado Plateau fauna investigated more wide-ranging species. These studies usually revealed low genetic diversity on the plateau, most often attributed to recent, and often multiple, colonization events (i.e. Douglas & Schuett, 2002; Leaché & Reeder, 2002; Mulcahy, 2008). Animals tended to have close genetic associations either with populations in the Great

Basin Desert in the west (Burbrink et al., 2011; Orange, Riddle, & Nickle, 1999; Wilson & Pitts, 2010) or the Chihuahuan Desert to the southeast (Bryson, De Oca, Jaeger, & Riddle, 2010; Haenel, 2007; Jaeger, Riddle, & Bradford, 2005). Research on two velvet ant species revealed that each contained a clade endemic to the Colorado Plateau, despite the fact that males of each species can fly (Wilson & Pitts, 2010, 2012). Furthermore, both studies identified potential glacial refugia in the plateau region that might be associated with lowlands in canyons. Here, we demonstrated that a less vagile arthropod species has persisted on the Mogollon Rim and in canyon-based refugia during the Pleistocene. This finding contributes to the emerging mixed nature of the Colorado Plateau fauna. Some animals recently colonized the region from adjacent deserts following the Last Glacial Maximum, while others, like tarantulas, persisted on the Mogollon Rim and expanded across the plateau from refugia in canyons.

ACKNOWLEDGEMENTS

BEH thanks Krissy Rehm and Thomas Martin for their assistance in the field; numerous citizen scientists who donated specimens; and Brendon Barnes for his assistance in the laboratory. MRG thanks Alexsis M. Powell for her help in the laboratory. Paula Cushing and Marshal Hedin graciously arranged for our training in library prep. Three anonymous reviewers and Rosemary Gillespie provided important comments that improved the manuscript. Funding for this project was provided by two Millsaps College Faculty Development Grants awarded to BEH and NSF grant DEB-1754030 awarded to MRG.

AUTHOR CONTRIBUTIONS

MRG and BEH designed the research. BEH collected the samples. MRG, CESL and BEH performed the laboratory work. All authors analysed the data and wrote the manuscript, with MRG leading.

DATA AVAILABILITY STATEMENT

Sampling locations, COI sequences: GenBank accession no. and RADseq data: GenBank Accession no. are provided in Table S1. Maxent input and ASC files: https://doi.org/10.5061/dryad.9zw3r22bj

ORCID

Matthew R. Graham https://orcid.org/0000-0001-7192-1083
Carlos E. Santibáñez-López https://orcid.org/0000-0001-6062-282X
Shahan Derkarabetian https://orcid.org/0000-0002-9163-9277
Brent E. Hendrixson https://orcid.org/0000-0003-1759-6405

REFERENCES

Angulo, D. F., Amarilla, L. D., Anton, A. M., & Sosa, V. (2017). Colonization in North American Arid lands: The journey of agarito (*Berberis trifoliolata*) revealed by multilocus molecular data and packrat midden fossil remains. *PLoS ONE*, *12*(2), e0168933. https://doi.org/10.1371/journal.pone.0168933

Avise, J. (2000). *Phylogeography: The History and Formation of Species*. Cambridge, MA: HarvardUniversity Press.

Bell, K. C., Hafner, D. J., Leitner, P., & Matocq, M. D. (2010). Phylogeography of the ground squirrel subgenus *Xerospermophilus* and assembly of the Mojave Desert biota. *Journal of Biogeography*, *37*(2), 363–378. https://doi.org/10.1111/j.1365-2699.2009.02202.x

Betancourt, J. L. (1990). Late quaternary biogeography of the Colorado Plateau. In J. L. Betancourt, T. R. Van Devender, & P. S. Martin (Eds.), *Packrat middens: The last, 40,000 years of biotic change* (pp. 259–292). Tucson, AZ: University of Arizona Press.

Bouckaert, R., Heled, J., Kühnert, D., Vaughan, T., Wu, C.-H., Xie, D., … Drummond, A. J. (2014). BEAST 2: A software platform for Bayesian evolutionary analysis. *PLoS Computational Biology*, *10*(4), e1003537. https://doi.org/10.1371/journal.pcbi.1003537

Boyer, S. L., Markle, T. M., Baker, C. M., Luxbacher, A. M., & Kozak, K. H. (2016). Historical refugia have shaped biogeographical patterns of species richness and phylogenetic diversity in mite harvestmen (Arachnida, Opiliones, Cyphophthalmi) endemic to the Australian Wet Tropics. *Journal of Biogeography*, *43*(7), 1400–1411. https://doi.org/10.1111/jbi.12717

Bryson Jr., R. W., De Oca, A. N. M., Jaeger, J. R., & Riddle, B. R. (2010). Elucidation of cryptic diversity in a widespread Nearctic treefrog reveals episodes of mitochondrial gene capture as frogs diversified across a dynamic landscape. *Evolution*, *64*(8), 2315–2330. https://doi.org/10.1111/j.1558-5646.2010.01014.x

Bryson Jr., R. W., Riddle, B. R., Graham, M. R., Smith, B. T., & Prendini, L. (2013). As old as the hills: Montane scorpions in southwestern North America reveal ancient associations between biotic diversification and landscape history. *PLoS ONE*, *8*(1), e52822. https://doi.org/10.1371/journal.pone.0052822

Burbrink, F. T., Yao, H., Ingrasci, M., Bryson Jr, R. W., Guiher, T. J., & Ruane, S. (2011). Speciation at the Mogollon Rim in the Arizona mountain kingsnake (*Lampropeltis pyromelana*). *Molecular Phylogenetics and Evolution*, *60*(3), 445–454. https://doi.org/10.1016/j.ympev.2011.05.009

Carnaval, A. C., Hickerson, M. J., Haddad, C. F., Rodrigues, M. T., & Moritz, C. (2009). Stability predicts genetic diversity in the Brazilian Atlantic forest hotspot. *Science*, *323*(5915), 785–789. https://doi.org/10.1126/science.1166955

Cather, S. M., Chapin, C. E., & Kelley, S. A. (2012). Diachronous episodes of Cenozoic erosion in southwestern North America and their relationship to surface uplift, paleoclimate, paleodrainage, and paleoaltimetry. *Geosphere*, *8*(6), 1177–1206. https://doi.org/10.1130/ges00801.1

Chattopadhyay, B., Garg, K. M., & Ramakrishnan, U. (2014). Effect of diversity and missing data on genetic assignments with RAD-Seq markers. *BMC Research Notes*, *7*, 841. https://doi.org/10.1186/1756-0500-7-841

Coats, L. L., Cole, K. L., & Mead, J. I. (2008). 50,000 years of vegetation and climate history on the Colorado Plateau, Utah and Arizona, USA. *Quaternary Research*, *70*(2), 322–338. https://doi.org/10.1016/j.yqres.2008.04.006

Cole, K. L., Fisher, J. F., Ironside, K., Mead, J. I., & Koehler, P. (2013). The biogeographic histories of *Pinus edulis* and *Pinus monophylla* over the last 50,000 years. *Quaternary International*, *310*, 96–110. https://doi.org/10.1016/j.quaint.2012.04.037

Coyle, F. A. (1983). Aerial dispersal by mygalomorph spiderlings (Araneae, Mygalomorphae). *Journal of Arachnology*, *11*, 283–286.

de Medeiros, B. A. S., & Farrell, B. D. (2018). Whole-genome amplification in double-digest RADseq results in adequate libraries but fewer sequenced loci. *PeerJ*, *6*, e5089. https://doi.org/10.7717/peerj.5089

Derkarabetian, S., Burns, M., Starrett, J., & Hedin, M. (2016). Population genomic evidence for multiple Pliocene refugia in a montane-restricted harvestman (Arachnida, Opiliones, *Sclerobunus robustus*) from the southwestern United States. *Molecular ecology*, *25*(18), 4611–4631. https://doi.org/10.1111/mec.13789

Devitt, T. J. (2006). Phylogeography of the Western Lyresnake (*Trimorphodon biscutatus*): Testing aridland biogeographical hypotheses across the Nearctic-Neotropical transition. *Molecular Ecology*, *15*, 4387–4407. https://doi.org/10.1111/j.1365-294X.2006.03015.x

Dolby, G. A., Dorsey, R. J., & Graham, M. R. (2019). A legacy of geo-climatic complexity and genetic divergence along the lower Colorado River: Insights from the geological record and 33 desert-adapted animals. *Journal of Biogeography*, *46*(11), 2479–2505. https://doi.org/10.1111/jbi.13685

Douglas, M. E., Douglas, M. R., Schuett, G. W., & Porras, L. W. (2006). Evolution of rattlesnakes (Viperidae; *Crotalus*) in the warm deserts of western North America shaped by Neogene vicariance and Quaternary climate change. *Molecular Ecology*, *15*, 3353–3374. https://doi.org/10.1111/j.1365-294X.2006.03007.x

Douglas, M. E., & Schuett, G. W. (2002). *Phylogeography of the western rattlesnake (*Crotalus viridis*) complex, with emphasis on the Colorado Plateau* (pp. 11–50). Eagle Mountain, UT: Eagle Mountain Pub.

Drummond, A. J., Suchard, M. A., Xie, D., & Rambaut, A. (2012). Bayesian phylogenetics with BEAUti and the BEAST 1.7. *Molecular Biology and Evolution*, *29*(8), 1969–1973. https://doi.org/10.1093/molbev/mss075

Dynesius, M., & Jansson, R. (2000). Evolutionary consequences of changes in species' geographical distributions driven by Milankovitch climate oscillations. *Proceedings of the National Academy of Sciences of the United States of America*, *97*(16), 9115–9120. https://doi.org/10.1073/pnas.97.16.9115

Earl, D. A., & vonHoldt, B. M. (2012). Structure harvester: A website and program for visualizing Structure output and implementing the Evanno method. *Conservation Genetics Resources*, *4*, 359–361. https://doi.org/10.1007/s12686-011-9548-7

Eaton, D. A. (2014). PyRAD: Assembly of de novo RADseq loci for phylogenetic analyses. *Bioinformatics*, *30*(13), 1844–1849. https://doi.org/10.1093/bioinformatics/btu121

Elith, J., Phillips, S. J., Hastie, T., Dudík, M., Chee, Y. E., & Yates, C. J. (2011). A statistical explanation of MaxEnt for ecologists. *Diversity and Distributions*, *17*(1), 43–57. https://doi.org/10.1111/j.1472-4642.2010.00725.x

Evanno, G., Regnaut, S., & Goudet, J. (2005). Detecting the number of clusters of individuals using the software Structure: A simulation study. *Molecular Ecology*, *14*, 2611–2620. https://doi.org/10.1111/j.1365-294x.2005.02553.x

Excoffier, L., Laval, G., & Schneider, S. (2005). Arlequin (version 3.0): An integrated software package for population genetics data analysis. *Evolutionary Bioinformatics*, *1*, 117693430500100003. https://doi.org/10.1177/117693430500100003

Fu, Y. X. (1997). Statistical tests of neutrality of mutations against population growth, hitchhiking and background selection. *Genetics*, *147*(2), 915–925.

Glenn, T. C., Bayona-Vasquez, N. J., Kieran, T. J., Pierson, T. W., Hoffberg, S. L., Scott, P. A., & Troendle, N. (2017). Adapterama III: Quadruple-indexed, triple-enzyme RADseq libraries for about $1 USD per Sample (3RAD). *bioRxiv*, 205799. https://doi.org/10.7717/peerj.7724

Graham, M. R., Hendrixson, B. E., Hamilton, C. A., & Bond, J. E. (2015). Miocene extensional tectonics explain ancient patterns of diversification among turret-building tarantulas (*Aphonopelma mojave* group) in the Mojave and Sonoran deserts. *Journal of Biogeography*, *42*(6), 1052–1065. https://doi.org/10.1111/jbi.12494

Graham, M. R., Jaeger, J. R., Prendini, L., & Riddle, B. R. (2013a). Phylogeography of the Arizona hairy scorpion (*Hadrurus arizonensis*) supports a model of biotic assembly in the Mojave Desert and adds a new Pleistocene refugium. *Journal of Biogeography*, *40*(7), 1298–1312. https://doi.org/10.1111/jbi.12079

Graham, M. R., Jaeger, J. R., Prendini, L., & Riddle, B. R. (2013b). Phylogeography of Beck's desert scorpion, *Paruroctonus becki*, reveals Pliocene diversification in the eastern California Shear Zone and postglacial expansion in the Great Basin Desert. *Molecular Phylogenetics and Evolution*, *69*(3), 502–513. https://doi.org/10.1016/j.ympev.2013.07.028

Graham, M. R., Wood, D. A., Henault, J. A., Valois, Z. J., & Cushing, P. E. (2017). Ancient lakes, Pleistocene climates and river avulsions structure the phylogeography of a large but little-known rock scorpion from the Mojave and Sonoran deserts. *Biological Journal of the Linnean Society*, *122*(1), 133–146. https://doi.org/10.1093/biolinnean/blx058

Graham, R. W., Lundelius, E. L., Graham, M. A., Schroeder, E. K., Toomey, R. S., Anderson, E., … Guthrie, R. D. (1996). Spatial response of mammals to late Quaternary environmental fluctuations. *Science*, *272*(5268), 1601–1606.

Haenel, G. J. (2007). Phylogeography of the tree lizard, *Urosaurus ornatus*: Responses of populations to past climate change. *Molecular Ecology*, *16*(20), 4321–4334. https://doi.org/10.1111/j.1365-294x.2007.03515.x

Hamilton, C. A., Formanowicz, D., & Bond, J. E. (2011). Species delimitation and phylogeography of *Aphonopelma hentzi* (Araneae, Mygalomorphae, Theraphosidae): Cryptic diversity in north american tarantulas. *PLoS ONE*, *6*(10), e26207. https://doi.org/10.1371/journal.pone.0026207

Hamilton, C. A., Hendrixson, B. E., & Bond, J. E. (2016). Taxonomic revision of the tarantula genus *Aphonopelma* Pocock, 1901 (Araneae, Mygalomorphae, Theraphosidae) within the United States. *ZooKeys*, *560*, 1–340. https://doi.org/10.3897/zookeys.560.6264

Hansen, J., Sato, M., Russell, G., & Kharecha, P. (2013). Climate sensitivity, sea level and atmospheric carbon dioxide. *Philosophical Transactions of the Royal Society A: Mathematical, Physical and Engineering Sciences*, *371*(2001), 20120294. https://doi.org/10.1098/rsta.2012.0294

Hedin, M. C., & Maddison, W. P. (2001). A combined molecular approach to phylogeny of the jumping spider subfamily Dendryphantinae (Araneae: Salticidae). *Molecular Phylogenetics and Evolution*, *18*(3), 386–403. https://doi.org/10.1006/mpev.2000.0883

Hedin, M., & McCormack, M. (2017). Biogeographical evidence for common vicariance and rare dispersal in a southern Appalachian harvestman (Sabaconidae, *Sabacon cavicolens*). *Journal of Biogeography*, *44*(7), 1665–1678. https://doi.org/10.1111/jbi.12973

Hendrixson, B. E. (2019). A new species of *Aphonopelma* (Araneae: Mygalomorphae: Theraphosidae) from the Madrean pine-oak woodlands of northeastern Sonora, Mexico. *Zootaxa*, *4688*(4), 519–534. https://doi.org/10.11646/zootaxa.4688.4.4

Hendrixson, B. E., DeRussy, B. M., Hamilton, C. A., & Bond, J. E. (2013). An exploration of species boundaries in turret-building tarantulas of the Mojave Desert (Araneae, Mygalomorphae, Theraphosidae, *Aphonopelma*). *Molecular Phylogenetics and Evolution*, *66*(1), 327–340. https://doi.org/10.1016/j.ympev.2012.10.004

Hendrixson, B. E., Guice, A. V., & Bond, J. E. (2015). Integrative species delimitation and conservation of tarantulas (Araneae, Mygalomorphae, Theraphosidae) from a North American biodiversity hotspot. *Insect Conservation and Diversity*, *8*, 120–131. https://doi.org/10.1111/icad.12089

Hereford, R. (2002). *Precipitation history of the Colorado Plateau region, 1900–2000*. US Department of the Interior, US Geological Survey. https://doi.org/10.3133/fs11902

Hijmans, R. J., Cameron, S. E., Parra, J. L., Jones, P., & Jarvis, A. (2005). Very high resolution interpolated climate surfaces for global land areas. *International Journal of Climatology*, *25*, 1965–1978. https://doi.org/10.1002/joc.1276

Hoang, D. T., Chernomor, O., von Haeseler, A., Minh, B. Q., & Vinh, L. S. (2018). UFBoot2: Improving the ultrafast bootstrap approximation. *Molecular Biology and Evolution*, *35*, 518–522. https://doi.org/10.1093/molbev/msx281

Hoffberg, S. L., Kieran, T. J., Catchen, J. M., Devault, A., Faircloth, B. C., Mauricio, R., & Glenn, T. C. (2016). RADcap: Sequence capture of

dual-digest RAD seq libraries with identifiable duplicates and reduced missing data. *Molecular Ecology Resources*, *16*(5), 1264–1278. https://doi.org/10.1111/1755-0998.12566

Huang, H., & Knowles, L. L. (2016). Unforeseen consequences of excluding missing data from Next-Generation sequences: Simulation study of RAD sequences. *Systematic Biology*, *65*, 357–365. https://doi.org/10.1093/sysbio/syu046

Huelsenbeck, J. P., & Ronquist, F. (2001). MRBAYES: Bayesian inference of phylogenetic trees. *Bioinformatics*, *17*, 754–755. https://doi.org/10.1093/bioinformatics/17.8.754

Jackobsson, M., & Rosenberg, N. A. (2007). Clumpp: A cluster matching and permutation program for dealing with label switching and multimodality in analysis of population structure. *Bioinformatics*, *23*, 1801–1806. https://doi.org/10.1093/bioinformatics/btm233

Jaeger, J. R., Riddle, B. R., & Bradford, D. F. (2005). Cryptic Neogene vicariance and Quaternary dispersal of the red-spotted toad (*Bufo punctatus*): Insights on the evolution of North American warm desert biotas. *Molecular Ecology*, *14*(10), 3033–3048. https://doi.org/10.1111/j.1365-294x.2005.02645.x

Janowski-Bell, M. E., & Horner, N. V. (1999). Movement of the male brown tarantula, *Aphonopelma hentzi* (Araneae, Theraphosidae) using radio telemetry. *Journal of Arachnology*, *27*, 503–512.

Jezkova, T., Jaeger, J. R., Marshall, Z. L., & Riddle, B. R. (2009). Pleistocene impacts on the phylogeography of the desert pocket mouse (*Chaetodipus penicillatus*). *Journal of Mammalogy*, *90*(2), 306–320. https://doi.org/10.1644/08-mamm-a-243.1

Jezkova, T., Olah-Hemmings, V., & Riddle, B. R. (2011). Niche shifting in response to warming climate after the last glacial maximum: Inference from genetic data and niche assessments in the chisel-toothed kangaroo rat (*Dipodomys microps*). *Global Change Biology*, *17*(11), 3486–3502. https://doi.org/10.1111/j.1365-2486.2011.02508.x

Jombart, T., Devillard, S., & Balloux, F. (2010). Discriminant analysis of principal components: A new method for the analysis of genetically structured populations. *BMC Genetics*, *11*(1), 94. https://doi.org/10.1186/1471-2156-11-94

Kalyaanamoorthy, S., Minh, B. Q., Wong, T. K. F., von Haeseler, A., & Jermiin, L. S. (2017). ModelFinder: Fast model selection for accurate phylogenetic estimates. *Nature Methods*, *14*, 587–589. https://doi.org/10.1038/nmeth.4285

Karlstrom, K. E., Coblentz, D., Dueker, K., Ouimet, W., Kirby, E., Van Wijk, J., … Donahue, M. S. (2012). Mantle-driven dynamic uplift of the Rocky Mountains and Colorado Plateau and its surface response: Toward a unified hypothesis. *Lithosphere*, *4*(1), 3–22. https://doi.org/10.1130/l150.1

Knowles, L. L. (2000). Tests of Pleistocene speciation in montane grasshoppers (genus *Melanoplus*) from the sky islands of western North America. *Evolution*, *54*(4), 1337–1348. https://doi.org/10.1111/j.0014-3820.2000.tb00566.x

Koizumi, I., Usio, N., Kawai, T., Azuma, N., & Masuda, R. (2012). Loss of genetic diversity means loss of geological information: The endangered Japanese crayfish exhibits remarkable historical footprints. *PLoS ONE*, *7*(3), e33986. https://doi.org/10.1371/journal.pone.0033986

Konar, A., Choudhury, O., Bullis, R., Fiedler, L., Kruser, J. M., Stephens, M. T., … Romero-Severson, J. (2017). High-quality genetic mapping with ddRADseq in the non-model tree *Quercus rubra*. *BMC Genomics*, *18*, 417. https://doi.org/10.1186/s12864-017-3765-8

Kumar, S., Stecher, G., Li, M., Knyaz, C., & Tamura, K. (2018). MEGA X: Molecular evolutionary genetics analysis across computing platforms. *Molecular Biology and Evolution*, *35*, 1547–1549. https://doi.org/10.1093/molbev/msy096

Lal, M. M., Southgate, P. C., Jerry, D. R., & Zenger, K. R. (2016). Fishing for divergence in a sea of connectivity: The utility of ddRADseq genotyping in a marine invertebrate, the black-lip pearl oyster *Pinctada margaritifera*. *Marine Genomics*, *25*, 57–68. https://doi.org/10.1016/j.margen.2015.10.010

Lamb, T., Jones, T. R., & Wettstein, P. J. (1997). Evolutionary genetics and phylogeography of tassel-eared squirrels (*Sciurus aberti*). *Journal of Mammalogy*, *78*(1), 117–133. https://doi.org/10.2307/1382645

Leaché, A. D., Banbury, B. L., Felsenstein, J., De Oca, A. N. M., & Stamatakis, A. (2015). Short tree, long tree, right tree, wrong tree: New acquisition bias corrections for inferring SNP phylogenies. *Systematic Biology*, *64*(6), 1032–1047. https://doi.org/10.1093/sysbio/syv053

Leaché, A. D., & Oaks, J. R. (2017). The utility of single nucleotide polymorphism (SNP) data in phylogenetics. *Annual Review of Ecology, Evolution, and Systematics*, *48*, 69–84. https://doi.org/10.1146/annurev-ecolsys-110316-022645

Leaché, A. D., & Reeder, T. W. (2002). Molecular systematics of the eastern fence lizard (*Sceloporus undulatus*): A comparison of parsimony, likelihood, and Bayesian approaches. *Systematic Biology*, *51*(1), 44–68. https://doi.org/10.1080/106351502753475871

Leigh, J. W., & Bryant, D. (2015). popart: Full-feature software for haplotype network construction. *Methods in Ecology and Evolution*, *6*(9), 1110–1116. https://doi.org/10.1111/2041-210x.12410

Licona-Vera, Y., Ornelas, J. F., Wethington, S., & Bryan, K. B. (2018). Pleistocene range expansions promote divergence with gene flow between migratory and sedentary populations of Calothorax hummingbirds. *Biological Journal of the Linnean Society*, *124*(4), 645–667. https://doi.org/10.1093/biolinnean/bly084

Loera, I., Ickert-Bond, S. M., & Sosa, V. (2017). Pleistocene refugia in the Chihuahuan Desert: The phylogeographic and demographic history of the gymnosperm Ephedra compacta. *Journal of Biogeography*, *44*(12), 2706–2716.

Massatti, R., & Knowles, L. L. (2014). Microhabitat differences impact phylogeographic concordance of codistributed species: Genomic evidence in montane sedges (*Carex* L.) from the Rocky Mountains. *Evolution*, *68*(10), 2833–2846. https://doi.org/10.1111/evo.12491

Masta, S. E. (2000). Phylogeography of the jumping spider *Habronattus pugillis* (Araneae: Salticidae): Recent vicariance of sky island populations? *Evolution*, *54*(5), 1699–1711. https://doi.org/10.1111/j.0014-3820.2000.tb00714.x

McQuarrie, N., & Chase, C. G. (2000). Raising the Colorado Plateau. *Geology*, *28*(1), 91–94. https://doi.org/10.1130/0091-7613(2000)028<0091:rtcp>2.3.co;2

Merow, C., Smith, M. J., & Silander Jr., J. A. (2013). A practical guide to MaxEnt for modeling species' distributions: What it does, and why inputs and settings matter. *Ecography*, *36*(10), 1058–1069. https://doi.org/10.1111/j.1600-0587.2013.07872.x

Minh, B. Q., Nguyen, M. A. T., & von Haeseler, A. (2013). Ultrafast approximation for phylogenetic bootstrap. *Molecular Biology and Evolution*, *30*, 1188–1195. https://doi.org/10.1093/molbev/mst024

Minin, V. N., Bloomquist, E. W., & Suchard, M. A. (2008). Smooth skyride through a rough skyline: Bayesian coalescent-based inference of population dynamics. *Molecular Biology and Evolution*, *25*(7), 1459–1471. https://doi.org/10.1093/molbev/msn090

Mitchell, S. G., & Ober, K. A. (2013). Evolution of *Scaphinotus petersi* (Coleoptera: Carabidae) and the role of climate and geography in the Madrean sky islands of southeastern Arizona, USA. *Quaternary Research*, *79*(2), 274–283. https://doi.org/10.1016/j.yqres.2012.11.001

Mulcahy, D. G. (2008). Phylogeography and species boundaries of the western North American Nightsnake (*Hypsiglena torquata*): Revisiting the subspecies concept. *Molecular Phylogenetics and Evolution*, *46*(3), 1095–1115. https://doi.org/10.1016/j.ympev.2007.12.012

Myers, E. A., Bryson Jr., R. W., Hansen, R. W., Aardema, M. L., Lazcano, D., & Burbrink, F. T. (2019). Exploring Chihuahuan Desert diversification in the gray-banded kingsnake, *Lampropeltis alterna* (Serpentes:

Colubridae). *Molecular Phylogenetics and Evolution*, *131*, 211–218. https://doi.org/10.1016/j.ympev.2018.10.031

Nguyen, L.-T., Schmidt, H. A., von Haeseler, A., & Minh, B. Q. (2014). IQ-TREE: A fast and effective stochastic algorithm for estimating maximum-likelihood phylogenies. *Molecular Biology Evolution*, *32*, 268–274. https://doi.org/10.1093/molbev/msu300

Ober, K., Matthews, B., Ferrieri, A., & Kuhn, S. (2011). The evolution and age of populations of *Scaphinotus petersi* Roeschke on Arizona Sky Islands (coleoptera, carabidae, cychrini). *ZooKeys*, *147*, 183. https://doi.org/10.3897/zookeys.147.2024

O'Connell, K. A., & Smith, E. N. (2018). The effect of missing data on coalescent species delimitation and a taxonomic revision of whipsnakes (Colubridae: *Masticophis*). *Molecular Phylogenetics and Evolution*, *127*, 356–366. https://doi.org/10.1016/j.ympev.2018.03.018

Orange, D. I., Riddle, B. R., & Nickle, D. C. (1999). Phylogeography of a wide-ranging desert lizard, *Gambelia wislizenii* (Crotaphytidae). *Copeia*, *1999*, 267–273. https://doi.org/10.2307/1447471

Papadopoulou, A., Anastasiou, I., & Vogler, A. P. (2010). Revisiting the insect mitochondrial molecular clock: The mid-Aegean trench calibration. *Molecular Biology and Evolution*, *27*(7), 1659–1672. https://doi.org/10.1093/molbev/msq051

Pederson, J. L., Mackley, R. D., & Eddleman, J. L. (2002). Colorado Plateau uplift and erosion evaluated using GIS. *GSA Today*, *12*(8), 4–10. https://doi.org/10.1130/1052-5173(2002)012<0004:cpuaae>2.0.co;2

Phillips, S. J., Anderson, R. P., & Schapire, R. E. (2006). Maximum entropy modeling of species geographic distributions. *Ecological Modelling*, *190*(3–4), 231–259. https://doi.org/10.1016/j.ecolmodel.2005.03.026

Pritchard, J. K., Stephens, M., & Donnelly, P. (2000). Inference of population structure using multilocus genotype data. *Genetics*, *155*, 945–959. https://doi.org/10.1111/j.1471-8286.2007.01758.x

Pritchard, J. K., Wen, X., & Falush, D. (2010). Documentation for structure software: Version 2.3. http://pritch.bsd.uchicago.edu/structure.html

Ramasamy, R. K., Ramasamy, S., Bindroo, B. B., & Naik, V. G. (2014). Structure plot: A program for drawing elegant structure bar plots in user friendly interface. *SpringerPlus*, *3*, 431. https://doi.org/10.1186/2193-1801-3-431

Rambaut, A. (2008). *FigTree vol 1.4.3*. Retrieved from http://tree.bio.ed.ac.uk/software/figtree

Rambaut, A., Drummond, A. J., Xie, D., Baele, G., & Suchard, M. A. (2018). Posterior summarization in Bayesian phylogenetics using Tracer 1.7. *Systematic Biology*, *67*, 901–904. https://doi.org/10.1093/sysbio/syy032

R Core Team (2017). *R: A language and environment for statistical computing*. Vienna, Austria: R Foundation for Statistical Computing. https://www.R-project.org

Reichling, S. B. (2000). Group dispersal in juvenile *Brachypelma vagans* (Araneae, Theraphosidae). *Journal of Arachnology*, *28*(2), 248–250. https://doi.org/10.1636/0161-8202(2000)028[0248:gdijbv]2.0.co;2

Ronquist, F., & Huelsenbeck, J. P. (2003). MRBAYES 3: Bayesian phylogenetic inference under mixed models. *Bioinformatics*, *19*, 1572–1574. https://doi.org/10.1093/bioinformatics/btg180

Ronquist, F., Teslenko, M., van der Mark, P., Ayres, D. L., Darling, A., Höhna, S., … Huelsenbeck, J. P. (2012). MRBAYES 3.2: Efficient Bayesian phylogenetic inference and model selection across a large model space. *Systematic Biology*, *61*, 539–542. https://doi.org/10.1093/sysbio/sys029

Shafer, A. B. A., Peart, C. R., Tusso, S., Maayan, I., Brelsford, A., Wheat, C. W., & Wolf, J. B. W. (2017). Bioinformatic processing of RAD-seq data dramatically impacts downstream population genetic inference. *Methods in Ecology and Evolution*, *8*, 907–917. https://doi.org/10.1111/2041-210x.12700

Smith, C. I., & Farrell, B. D. (2005). Phylogeography of the longhorn cactus *beetle Moneilema appressum* LeConte (Coleoptera: Cerambycidae): Was the differentiation of the Madrean sky islands driven by Pleistocene climate changes? *Molecular Ecology*, *14*(10), 3049–3065. https://doi.org/10.1111/j.1365-294X.2005.02647.x

Stoltey, T., & Shillington, C. (2009). Metabolic rates and movements of the male tarantula *Aphonopelma anax* during the mating season. *Canadian Journal of Zoology*, *87*(12), 1210–1220. https://doi.org/10.1139/Z09-111

Tajima, F. (1989). Statistical method for testing the neutral mutation hypothesis by DNA polymorphism. *Genetics*, *123*(3), 585–595.

Thomas, S. M., & Hedin, M. (2008). Multigenic phylogeographic divergence in the paleoendemic southern Appalachian opilionid *Fumontana deprehendor* Shear (Opiliones, Laniatores, Triaenonychidae). *Molecular Phylogenetics and Evolution*, *46*(2), 645–658. https://doi.org/10.1016/j.ympev.2007.10.013

Toews, D. P., & Brelsford, A. (2012). The biogeography of mitochondrial and nuclear discordance in animals. *Molecular Ecology*, *21*(16), 3907–3930. https://doi.org/10.1111/j.1365-294x.2012.05664.x

Wagner, C. E., Keller, I., Wittwer, S., Selz, O. M., Mwaiko, S., Greuter, L., … Seehausen, O. (2013). Genome-wide RAD sequence data provide unprecedented resolution of species boundaries and relationships in the Lake Victoria cichlid adaptive radiation. *Molecular Ecology*, *22*(3), 787–798. https://doi.org/10.1111/mec.12023

Warren, D. L., Glor, R. E., & Turelli, M. (2010). ENMTools: A toolbox for comparative studies of environmental niche models. *Ecography*, *33*, 607–611. https://doi.org/10.1111/j.1600-0587.2009.06142.x

Wilson, J. S., & Pitts, J. P. (2010). Phylogeographic analysis of the nocturnal velvet ant genus *Dilophotopsis* (Hymenoptera: Mutillidae) provides insights into diversification in the Nearctic deserts. *Biological Journal of the Linnean Society*, *101*(2), 360–375. https://doi.org/10.1111/j.1095-8312.2010.01526.x

Wilson, J. S., & Pitts, J. P. (2012). Identifying Pleistocene refugia in North American cold deserts using phylogeographic analyses and ecological niche modelling. *Diversity and Distributions*, *18*(11), 1139–1152. https://doi.org/10.1111/j.1472-4642.2012.00902.x

SUPPORTING INFORMATION

Additional supporting information may be found online in the Supporting Information section.

How to cite this article: Graham MR, Santibáñez-López CE, Derkarabetian S, Hendrixson BE. Pleistocene persistence and expansion in tarantulas on the Colorado Plateau and the effects of missing data on phylogeographical inferences from RADseq. *Mol Ecol*. 2020;00:1–18. https://doi.org/10.1111/mec.15588